FABRICATION OF TRANSISTORS FROM PURIFIED $(7, 6)$ CARBON NANOTUBES

by

David Alan Jones

A senior thesis submitted to the faculty of

Brigham Young University

in partial fulfillment of the requirements for the degree of

Bachelor of Science

Department of Physics and Astronomy

Brigham Young University

August 2009

BRIGHAM YOUNG UNIVERSITY

DEPARTMENT APPROVAL

of a senior thesis submitted by

David Alan Jones

This thesis has been reviewed by the research advisor, research coordinator, and department chair and has been found to be satisfactory.

Date	Dr. Robert Davis, Advisor
Date	Eric Hintz, Research Coordinator
Date	Ross L. Spencer, Chair

ABSTRACT

FABRICATION OF TRANSISTORS FROM PURIFIED $(7, 6)$ CARBON NANOTUBES

David Alan Jones

Department of Physics and Astronomy

Bachelor of Science

We present a scalable procedure for the fabrication of transistors from purified $(7, 6)$ carbon nanotubes. CoMoCAT nanotubes are purified via isopycnic centrifugation and dielectrophoretically placed between electrodes. The resultant devices display on/off ratios as high as 10^3 and resistances as low as 10^6. Approximately 50% of all the devices display an on/off ratio greater than 10. The potential for higher yields is discussed.

ACKNOWLEDGMENTS

I would like to thank my wife, Sarah, for her support throughout this project, Hiram Conley for his role as my mentor, Brian Davis for his assistance with electrical measurements, Dr. Robert Davis for his general guidance, and the National Science Foundation for their financial support (CBET 0708347).

Contents

List of Figures

Chapter 1

Introduction

As the semiconductor industry marches towards nanoscale electronics, the carbon nanotube is becoming an increasingly important prospect for new innovations, promising smaller size, faster speeds[4] and lower power consumption.[5] As with all novel discoveries, however, there are challenges that must first be overcome. In this chapter, we begin with an overview of the properties of carbon nanotubes. We then introduce the fundamental problems associated with carbon nanotube transistors along with our proposed solutions.

1.1 The Single-walled Carbon Nanotube

The single-walled carbon nanotube, a member of the fullerene family, is a hollow, cylindrical carbon structure often described as a rolled-up sheet of graphene (see Figure 1.1). As opposed to the multi-walled carbon nanotube, which has several concentric layers, the single-walled carbon nanotube has only one, making it the simpler case for extensive study. (In this document, the word *nanotube* refers to single-walled carbon nanotubes exclusively). In Figure 1.1(b), the carbon atoms,

represented by spheres, appear to curl around the axis of the nanotube, forming a helix-like structure. This curl, called chirality, is used to differentiate one nanotube species from another.

Chirality is best understood from a two-dimensional chirality diagram, as in Figure 1.2. Given a graphene grid, a chirality diagram can be drawn by choosing an origin (shown as a red dot in Figure 1.2) and identifying the directions of the unit vectors $\hat{\vec{a}}_1$ and $\hat{\vec{a}}_2$ (shown as green arrows). The vectors $n\vec{a}_1$ and $m\vec{a}_2$ can then be drawn, the former starting from the origin and the latter starting from the tip of the former. The variables n and m are integers that compose the chiral index, notated as (n, m) with $n > m$. In Figure 1.2, $(n, m) = (7, 6)$, so these vectors become $7\vec{a}_1$ and $6\vec{a}_2$ (shown as blue arrows). The chiral vector $\vec{R} = n\vec{a}_1 + m\vec{a}_2$ may then be drawn using the principles of vector addition. The chiral vector represents the circumference of the nanotube. Lines drawn perpendicular to the chiral vector represent the ends that would meet if the graphene sheet could be cut out and connected. If these perpendicular lines are extended to the point where the carbon pattern enclosed begins to repeat itself, then a unit cell is defined. In Figure 1.2, the unit cell is the area enclosed by red lines. The unit cell is the smallest entity that fully describes the nature of a particular nanotube species. A single nanotube usually contains thousands of unit cells.

Fundamental properties about a particular nanotube species can be determined from its chirality. Conductivity, for example, is a function of the chiral indices m and n: if $(n - m)/3$ is an integer, then the species is metallic; otherwise, it is semiconducting.[6] The primary obstacle of nanotube electronics is the even dispersement of metallic species among semiconducting species (see Figure 1.3).

The radius r of a nanotube is also a function of the chiral indices:

$$r(m, n) = \frac{\sqrt{3}}{2\pi} a \sqrt{(m^2 + mn + n^2)}, \tag{1.1}$$

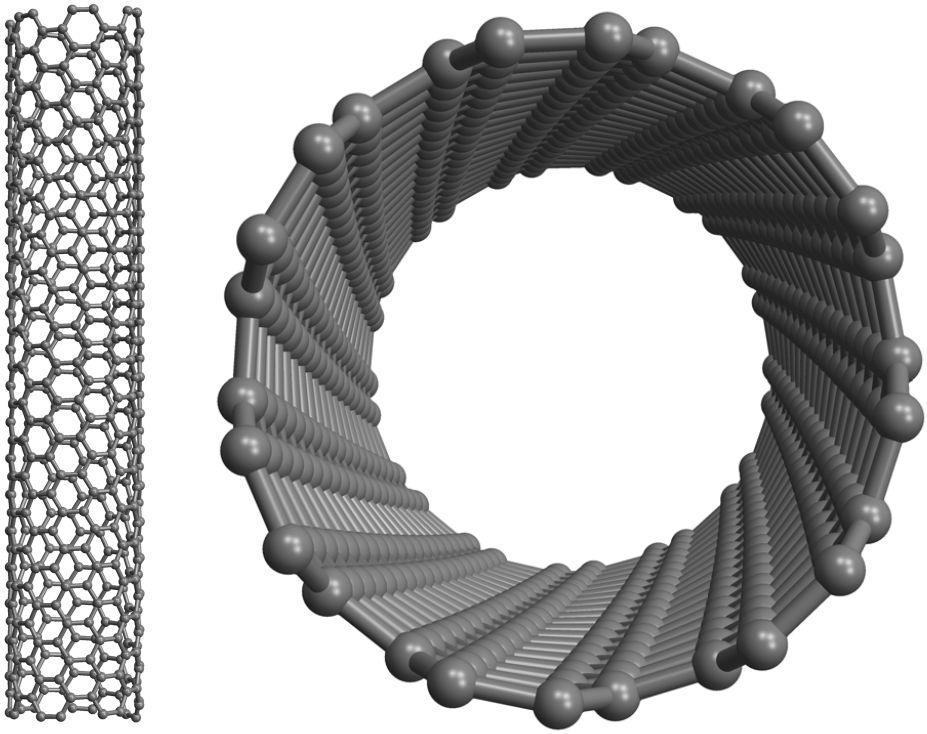

(a) (b)

Figure 1.1 A ball-and-stick model showing (a) a side view and (b) an axial view of a $(7, 6)$ single-walled carbon nanotube. Notice in (b) how the carbon atoms, represented by spheres, tend to curl around the axis. This curl, called chirality, differentiates one nanotube species from another. The coordinate file was produced by TubeVBS[11] and rendered with Mathematica.[12]

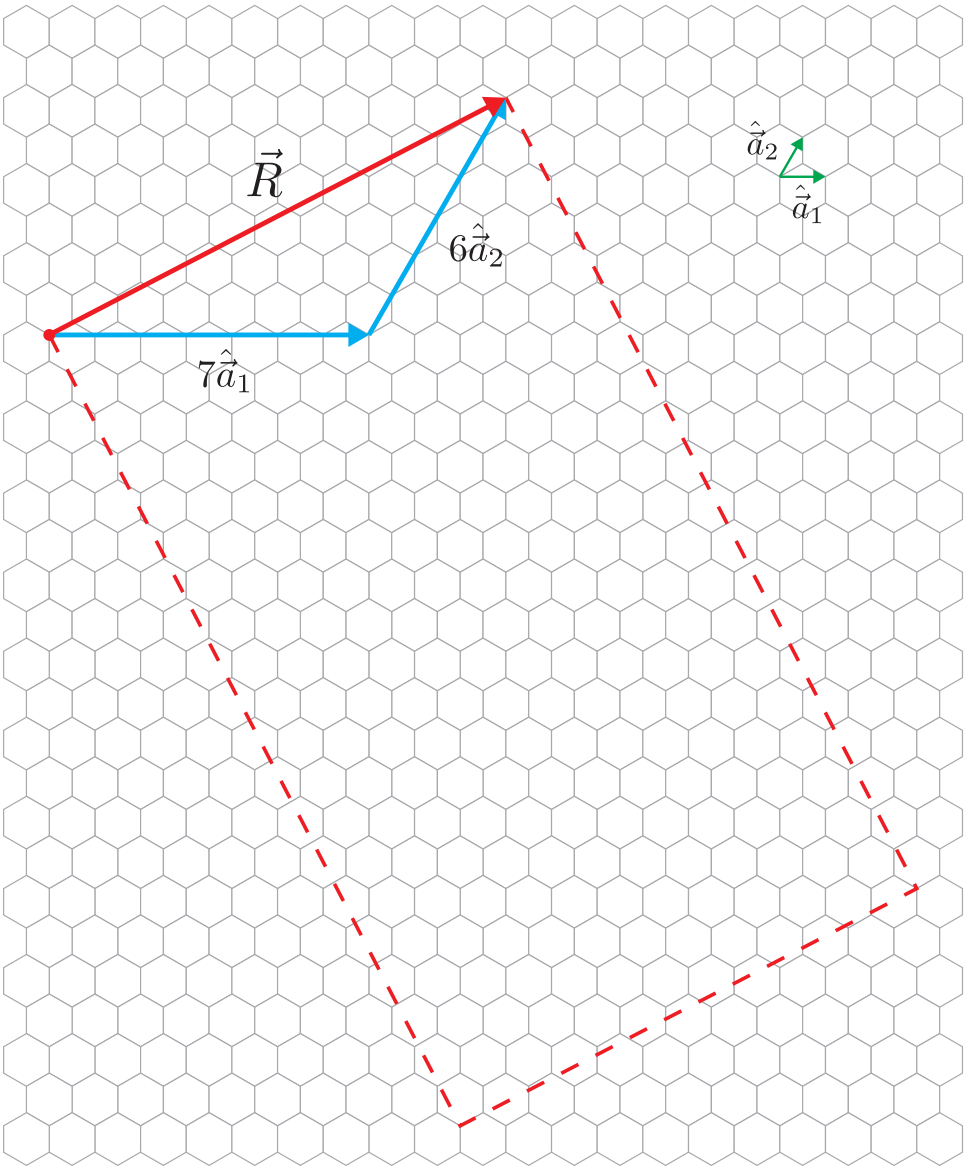

Figure 1.2 A two-dimensional chirality diagram of a $(7, 6)$ nanotube. The vectors $7\vec{a}_1$ and $6\vec{a}_2$ are drawn tip-to-tail from the origin. Vector addition yields the chiral vector $\vec{R} = 7\vec{a}_1 + 6\vec{a}_2$, which represents the circumference of the nanotube. A unit cell, shown here as dashed red lines, is formed by extending lines parallel to R to a point where the pattern enclosed begins to repeat itself.

where the constant $a = 0.142$ nm is the bond length between carbon atoms.[9] Knowing the radius, we can also derive the density of an isolated nanotube in vacuum:

$$\rho_n(r) = \frac{m_n}{V_n} = \frac{(2\pi r)l\sigma_g}{(\pi r^2)l} = \frac{2\sigma_g}{r} \tag{1.2}$$

where the variables m_n, V_n, and l represent the mass, volume, and length of the nanotube and the constant $\sigma_g = 7.663 \times 10^{-8}$ g/cm^2 is the surface density of graphene. Although this formula may not be useful in the laboratory, the inverse proportionality of radius with density allows a relationship to be drawn between *chirality* and density.

1.2 Purification via Isopycnic Centrifugation

Nanotubes will not prove useful in the field of nanoelectronics until they can be separated by their electrical properties, or equivalently, by their radius or density. Although there are many proposed methods for nanotube purification, we only address isopycnic centrifugation in an effort to show that a single scalable method is capable of producing high yields of operating nanotube transistors. Ultimately, however, it is likely that a combination of purification techniques will prove most effective.[7]

Isopycnic centrifugation has been shown to be an effective means of isolating certain species of nanotubes.[1] The word *isopycnic* originates from the Greek words *iso-*, meaning equal, and *pyknós*, meaning dense. Isopycnic centrifugation can be understood in terms of inertia, the tendency for matter to resist acceleration. When a particle is subject to constant circular motion, it experiences centripetal acceleration (since Δv points towards the center of rotation). The inherent inertia of the particle, measured in terms of mass, causes the particle to resist this acceleration, which results in centrifugal motion. Thus, a particle with greater mass has a greater tendency to move away from the center of rotation. This principle is much the same for the collection of particles that compose a liquid, but in the case of a liquid, inertia is

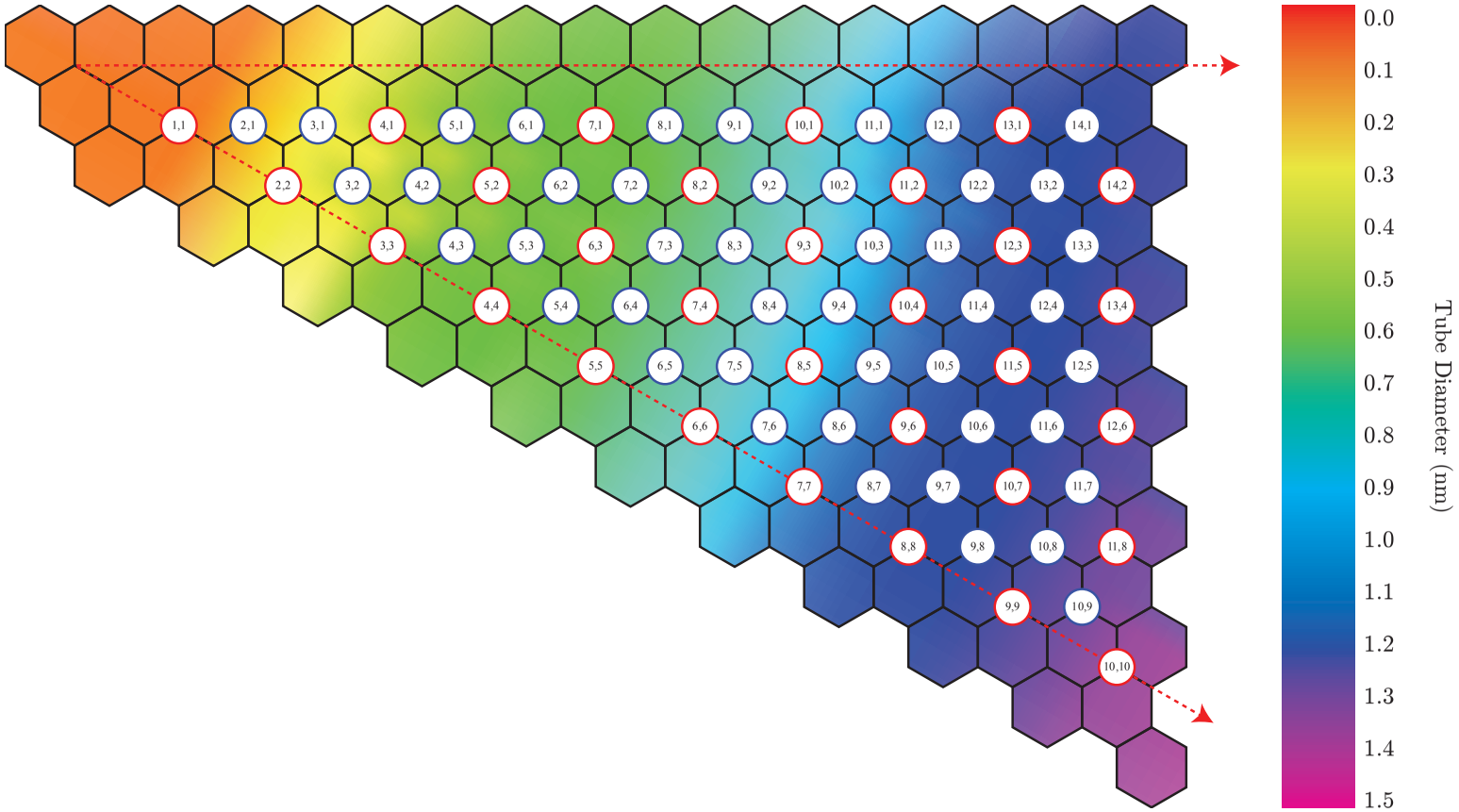

Figure 1.3 A chirality map. Each circle represents a unique chiral index (m, n). A line drawn from the origin to the center of any circle is equivalent to the chiral vector, thus representing the circumference of the corresponding nanotube structure. Red circles indicate metallic species, while blue circles indicate semiconducting species. The diameter (and thus density) of each species is indicated by the color scale. Notice the even dispersement of metallic species among semiconducting species.

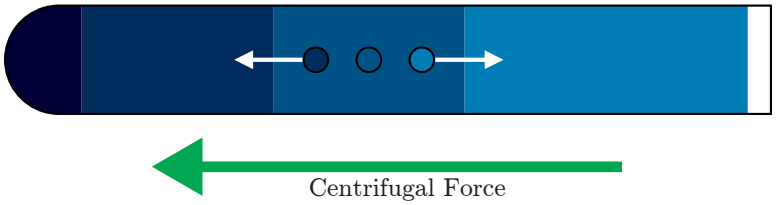

Figure 1.4 A side view of a centrifuge tube under centrifugal force. Particles are mobilized until they reach their isopycnic points.

measured in terms of mass per unit volume. Thus, in a liquid, a particle with greater *density* has a greater tendency to move away from the center of rotation.

In isopycnic centrifugation, various layering techniques are used to create a density gradient within a centrifuge tube. Under the centrifugal force, any given fraction of the gradient will remain stationary, since the layer just below it has greater density and thus greater inertia. Such a fraction, which is no longer mobile, is said to have reached its isopycnic point. If a particle is inserted into a region of low density, its own inertia will cause it to move further away from the center of rotation. If a particle is inserted into a region of high density, it will be displaced by particles with greater inertia. Thus, any particle, when inserted into a density gradient and subjected to a centrifugal force, becomes mobile and remains so until it reaches its isopycnic point, where it remains at equilibrium (see Figure 1.4).

In this study, nanotubes are dispersed in an aqueous solution and inserted into a continuous density gradient. When subjected to a centrifugal force, each species finds equilibrium at a unique isopycnic point, since each has a unique density. Thus, spatial separation between species is achieved. In practice, this spatial separation is manifested by thin bands which form within the centrifuge tube, each distinguishable by unique coloration. These bands may then be extracted and isolated with a commercial fractionator.

1.3 Placement via Dielectrophoresis

A carbon nanotube, even when isolated according to its electrical properties, is of no use in nanoelectronics unless it can be appropriately placed into a circuit. The most promising method of such controlled placement is dielectrophoresis.

When a dielectric particle is placed in any field, a dipole is induced in the particle, causing it to react to the field. In a uniform field, this reaction is manifested as rotational motion; the particle will rotate until its dipole moment is aligned with the field, at which point it ceases to move. In a nonuniform field, however, the particle will experience both rotational *and* translational motion. The phenomenon which causes this translation-inducing force in a non-uniform field is known as dielectrophoresis. If the electric field is well designed, this effect can be used to place the particle at any desired location.

Since the dielectrophoretic effect has no regard for polarity, it can operate under both direct and alternating currents. In cases where the particle may carry a slight charge, an alternating current will prevent excessive translational motion associated with standard electrophoresis. In our case, the surfactant-encapsulated nanotubes *do* carry a slight charge, so we use alternating current.

In this study, an alternating current is driven between opposing gold electrodes, which are submerged in water. The geometry of the electrodes is such that a nonuniform electric field is produced (see Figure 1.5). When nanotube solution is inserted above the electrodes, the dielectrophoretic force traps a nanotube between them, creating a carbon nanotube transistor.

It has been shown that dielectrophoresis, when performed at particular frequencies, may have preference for carbon nanotubes of one electrical type over another, providing further purification of nanotube species.[8] Thus, when used together, isopy-

cnic centrifugation and dielectrophoresis may provide a complete solution to nanotube purification and placement.

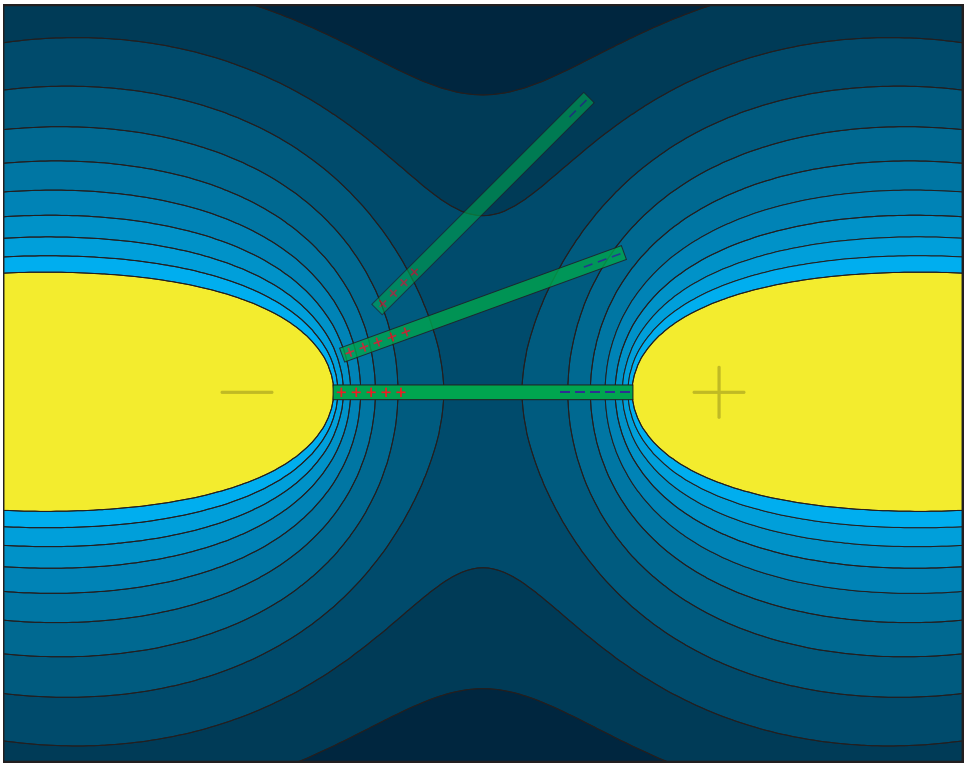

Figure 1.5 A nanotube being trapped via dielectrophoresis. A voltage is applied between two electrodes (gold), which creates a nonuniform electric field in water (blue). Lighter shades of blue represent stronger areas of the field. The electric field induces a dipole in a randomly placed nanotube, whose ends are then attracted to the electrodes. The fact that the field is nonuniform allows for both rotational *and* translational motion of the nanotube. (If the field were uniform, the nanotube would simply rotate into an equilibrium state and cease to be mobile.) Note that the dielectrophoretic effect is the same regardless of polarity.

Chapter 2

Methods

2.1 Purification

The nanotubes used in this study are grown via the CoMoCAT^2 method, which produces a course powder of entangled nanotube aggregates. In preparation for isopycnic centrifugation, these aggregates must be disaggregated and dissolved into solution. To achieve this, the nanotubes are dispersed into a solution of surfactant-enriched water, which is then sonicated with a horn sonicator. The surfactants, which include sodium cholate and sodium dodecyl sulfate, have both hydrophilic and hydrophobic ends, allowing one end to adsorb to the nanotube while the other end adsorbs to a solvent molecule. Once the nanotubes are disaggregated via sonic disruption, the surfactants prevent neighboring nanotubes, which are weakly attracted to each other, from reaggregating. Thus, a stable, homogeneous nanotube solution is achieved.

Following sonication, catalyst and remaining nanotube aggregates are removed by directly centrifuging the decanted nanotube solution for a short period of time. This method, called differential centrifugation, does not utilize a density gradient, allowing the most massive particles to sediment relatively quickly. As sedimentation

progresses, a solid pellet of nanotube aggregate forms at the bottom of the centrifuge tube. This process is referred to as pelletization. After pelletization is complete, the supernatant is decanted for further processing.

Since any given nanotube moves very slowly through the density gradient, it is important to minimize the distance between its initial position and its isopycnic point. To achieve this, the nanotube solution is concentrated using isopycnic centrifugation with a discrete 2-step density gradient. The discrete gradient is formed by layering the decanted nanotube solution over a layer of OptiPrep, the density gradient medium used throughout this study. The bottom step acts as a barrier, causing highly concentrated nanotube solution to band at the interface. The resulting band, usually less than 1 mL of solution, is then fractionated using a commercial fractionator.

With the nanotube solution properly homogenized and concentrated, it is fully prepared for separation. In contrast with the concentration step, which utilizes a discrete density gradient, the separation step utilizes a *continuous* density gradient (see Figure 2.1). This provides the resolution necessary to resolve the small density differences between nanotube species. A continuous density gradient is formed by layering several steps of decreasingly dense OptiPrep in a centrifuge tube. The concentrated nanotube solution is also layered into the gradient, often near its center. In an effort to create a convex gradient, the topmost step is made larger than the bottommost step. A convex gradient causes high-density particles to sediment more quickly while increasing the resolution of low-density particles. Other gradient shapes may have advantages over the one used here, but alternatives were not studied comprehensively. In order to properly balance the centrifuge rotor, another density gradient is prepared by the same procedure in a second centrifuge tube. The centrifuge tubes are then sealed with Parafilm and laid on their sides; this increases the surface area of each layer and accelerates the rate of diffusion between them. When the density gradients

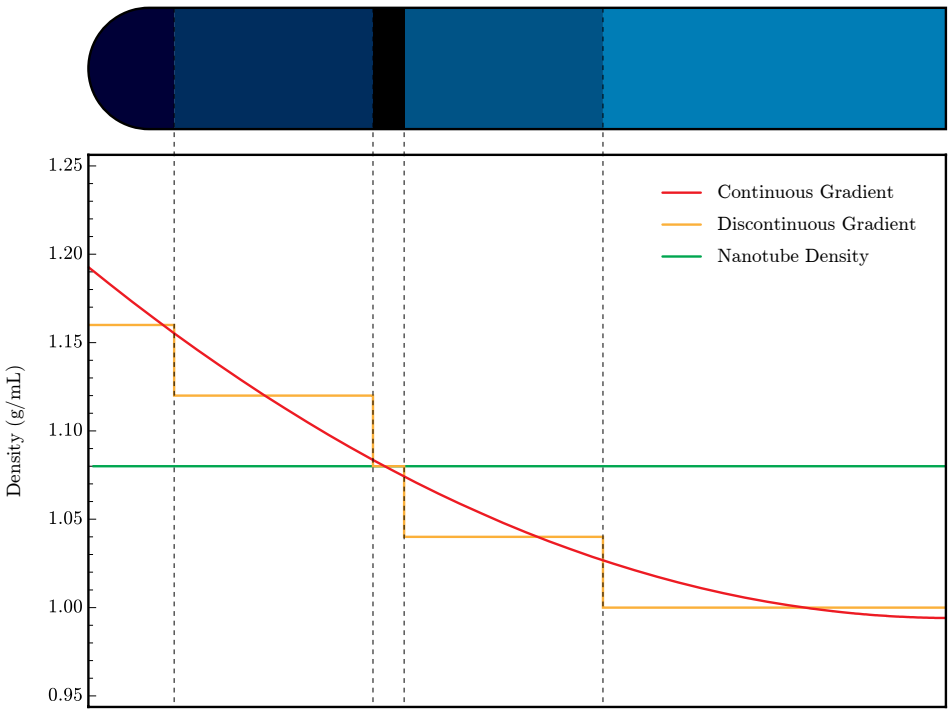

Figure 2.1 The density gradient profile used in this study. Lighter shades of blue represent lower densities while darker shades of blue represent higher densities. The discontinuous gradient is centered around the density of the nanotube fraction, shown here as a black band in the centrifuge tube. After two hours of diffusion, the gradient becomes approximately continuous, able to resolve the fine density differences between nanotube species.

are approximately continuous, they are each inserted into opposing sides of the rotor and centrifuged until the desired nanotube species form coherent bands at their isopycnic points.

When isopycnic centrifugation is complete, the centrifuge tubes are immediately removed and inserted into a commercial fractionator. The trumpet of the fractionator is lowered to the first band and fractions are taken in steps of 0.5 mm. Since the surfactants cause a great deal of foaming during the fractionation process, each fraction is briefly centrifuged in a tabletop centrifuge, causing the foam to condense into liquid. About 40 fractions are produced for each centrifuge tube.

2.2 Absorption Spectroscopy

Any given nanotube species has several characteristic absorption peaks resulting from transitions which occur between van Hove singularities in its density of states.[10] These peaks have corresponding energies E_{11}, E_{22}, etc., with wavelengths λ_{11}, λ_{22}, etc. After the nanotube fractions are collected, they are each analyzed in the visible and near-infrared ranges with a spectrophotometer. The λ_{11} and λ_{22} peaks are identified and compared to known values and their associated species (see Table 2.1).[3] The fraction with the highest population of $(7, 6)$ species is identified and selected for electrical studies.

2.3 Dielectrophoresis

In preparation for dielectrophoresis, arrays of opposing gold electrodes are prepared on a silicon oxide chip using electron beam lithography. Each electrode connects to a relatively large gold pad, making it possible to create electrical contact using

λ_{11}	λ_{22}	Chirality	λ_{11}	λ_{22}	Chirality
833	483	(5,4)	1250	786	(10,5)
873	581	(6,4)	1263	611	(11,1)
912	693	(9,1)	1267	728	(8,7)
952	663	(8,3)	1307	859	(13,2)
975	567	(6,5)	1323	790	(9,7)
1023	644	(7,5)	1342	857	(12,4)
1053	734	(10,2)	1372	714	(11,4)
1101	720	(9,4)	1376	685	(12,2)
1113	587	(8,4)	1380	756	(10,6)
1122	647	(7,6)	1397	858	(11,6)
1139	551	(9,2)	1414	809	(9,8)
1171	797	(12,1)	1425	927	(15,1)
1172	716	(8,6)	1474	868	(10,8)
1197	792	(11,3)	1485	928	(13,5)
1244	671	(9,5)	1496	795	(12,5)
1250	633	(10,3)	1497	760	(13,3)

Table 2.1 Characteristic absorption wavelengths and their associated chiralities. Adapted from Bachilo et al.[3]

micromanipulator tips. A diamond-tip scribe is then used to scratch a small hole through the oxide; this allows access to the underlying silicon, which will be used as a back-gate during the electrical measurements. The chip is then gently washed in preparation for the next step.

The chip is placed in a petri dish, which is then filled with water. Micromanipulator tips are lowered onto opposing electrodes and a 50,000 Hz alternating current of 8-20 V (peak to peak) is produced between them using a sine function generator. Approximately 50 μL of nanotube solution is then dropped directly above the electrodes. At this point, dielectrophoresis is taking place and is allowed approximately one minute to trap a nanotube. This process is repeated for several pairs of electrodes, moving the micromanipulator tips to a new set of pads before each iteration.

When dielectrophoresis is complete, the chip is gently washed by flowing water into one side of the petri dish while allowing it to drain from the other side. This process removes excess surfactant molecules from the surface of the chip. In order to remove the surfactant molecules from the nanotubes themselves, the chip is annealed overnight at 100 C.

2.4 Electrical Measurements

In preparation for electrical measurements, three micromanipulator tips are connected to a data acquisition interface; in this study, LabVIEW is used with the virtual instrument meaSureit. Two micromanipulator tips are then lowered onto the source and drain of a single device, while the third tip is lowered onto the previously prepared hole in the oxide (the back-gate). The software applies a voltage to the source while collecting data from the drain.

Source voltage sweeps are performed by varying the voltage between -1 V and 1 V

while maintaining a constant gate voltage of -4 V, 0 V, or 4 V; the back-gate voltage is adjusted prior to each sweep in an effort to detect gate dependence. Additionally, gate voltage sweeps are performed by maintaining a constant source-drain voltage (typically less than 1 V) and sweeping the gate voltage between -5 V and 5 V.

Chapter 3

Results

When isopycnic centrifugation was complete, distinct bands were visible near the center of the centrifuge tube (see Figure 3.1). Contrary to intuition, absorption spectroscopy of the resultant fractions shows that nanotube species with smaller radii (greater densities) settle near the top of the gradient, while species with larger radii (lesser densities) settle near the bottom.

Each subsequent fraction presented only slight optical absorption differences from its neighbor, with characteristic peaks slowly increasing, reaching a maximum value, and then slowly decreasing. The width of the $(6, 5)$ distribution is much smaller than the distance between the $(6, 5)$ and $(7, 6)$ maxima, which indicates that the two species were effectively isolated from each other (see Figure 3.2). Notable fractions were numbers 10 and 25, which had relatively large populations of $(6, 5)$ and $(7, 6)$ species, respectively (see Figure 3.3). Due to its large population of $(7, 6)$ species, fraction 25 was used in all electrical measurements.

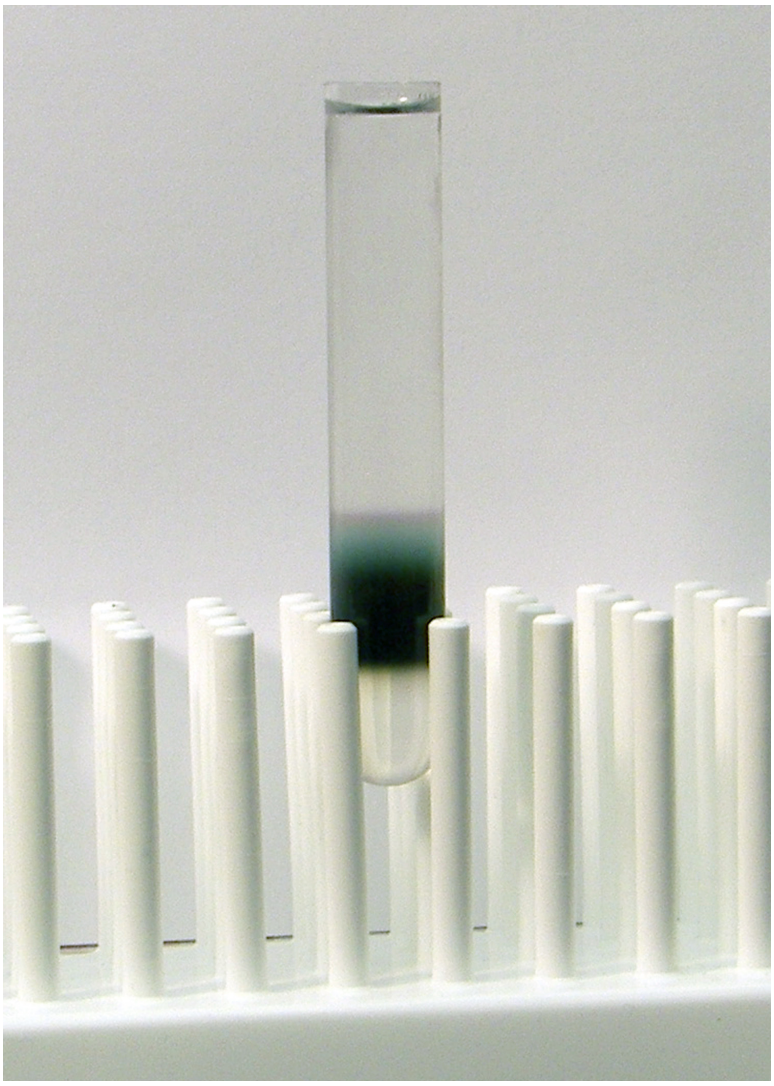

Figure 3.1 A centrifuge tube after the separation step. There are three distinct band colors: pink, green, and black. The pink band consists primarily of $(6, 5)$ species while the green band consists primarily of $(7, 6)$ species. The black band consists of larger-radius species and aggregates.

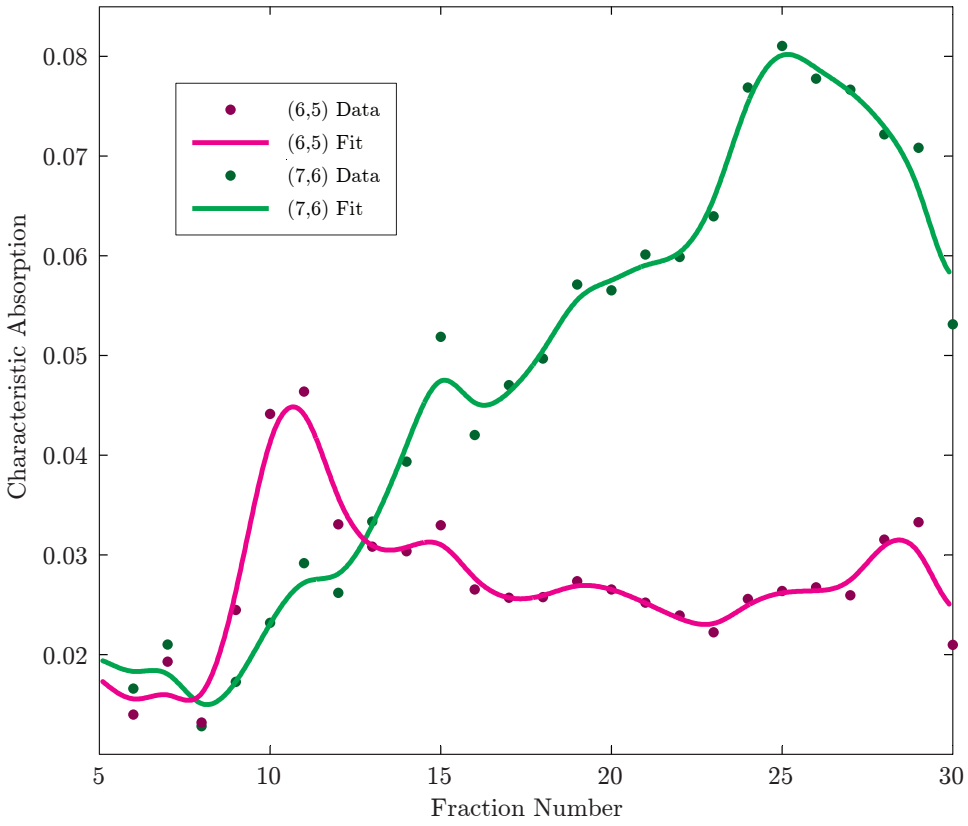

Figure 3.2 The distribution of $(6,5)$ and $(7,6)$ species throughout the density gradient. The width of the $(6,5)$ distribution is much smaller than the distance between the $(6,5)$ and $(7,6)$ maxima, which indicates that the two species were effectively isolated from each other.

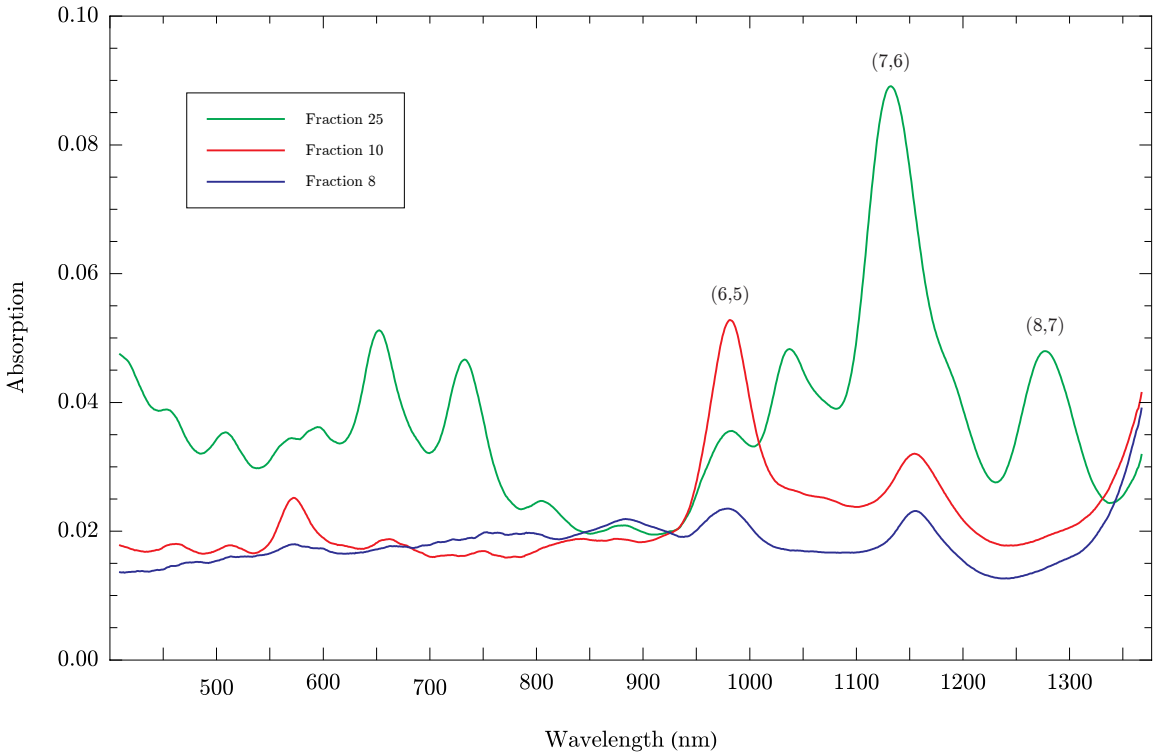

Figure 3.3 An overlay of three absorption plots. Fraction 25, shown here in green, is highly enriched with $(7, 6)$ species.

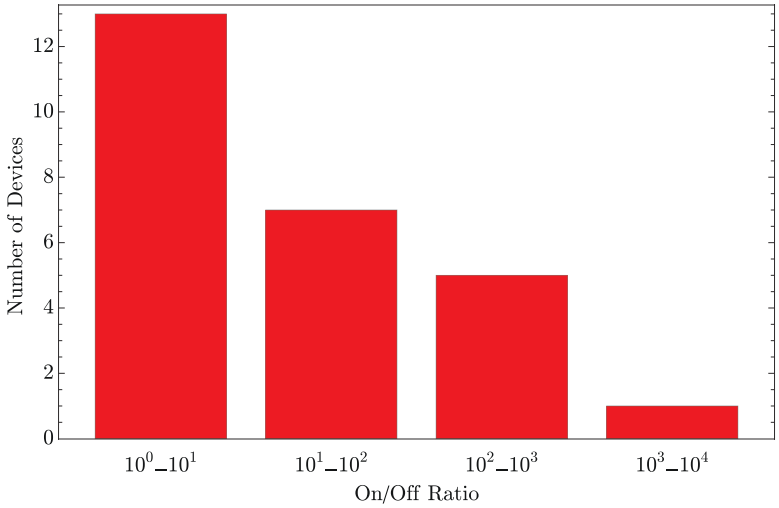

Figure 3.4 A histogram of transistor devices with respect to on/off ratio.

Of the 35 transistor devices that were fabricated, 4 were found to have no current, 4 were found to have abnormal electrical properties, and 1 stopped conducting during measurement, leaving a total of 26 devices for this study. The resultant devices displayed on/off ratios as high as 10^3 and resistances as low as 10^6. Approximately 50% of all the devices displayed an on/off ratio greater than 10 (see Figure 3.4). Gate voltage sweeps, such as that in Figure 3.5, show the semiconducting nature of the devices. Source voltage sweeps of the devices resulted in plots similar to Figure 3.6, but many did not display such symmetry, with their centers shifted to the left or right. In some cases, this resulted in below-average on/off ratios. Table 3.1 shows detailed information for each device.

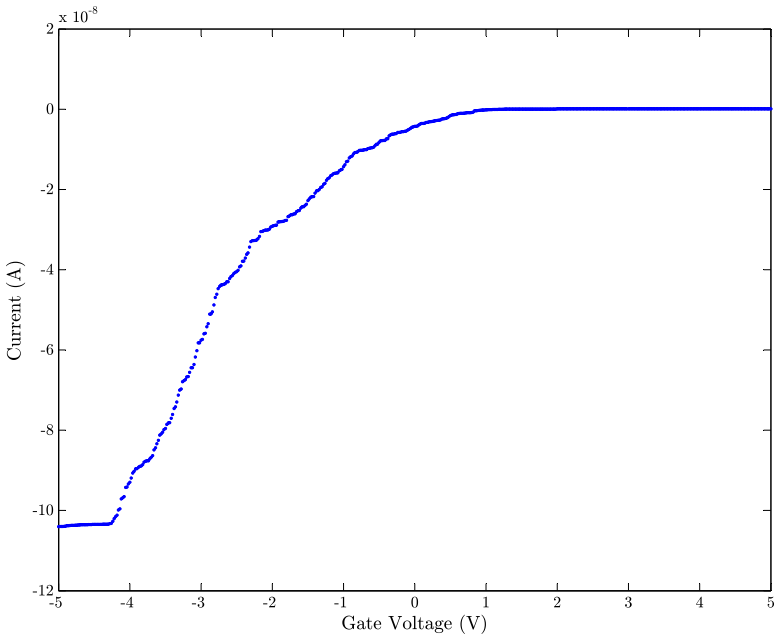

Figure 3.5 A gate voltage sweep of Device 11 with a source-drain voltage of -1 V.

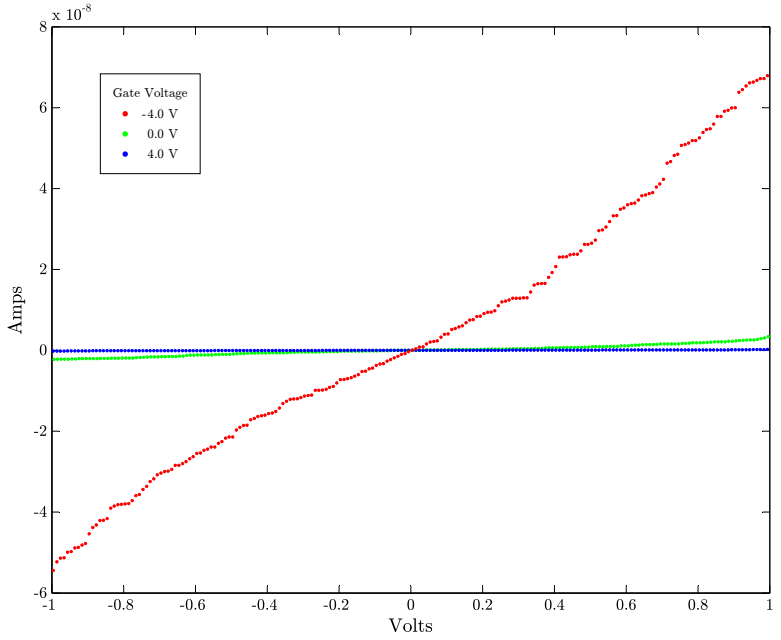

Figure 3.6 A source voltage sweep of Device 23 with three levels of back-gating, displaying an on/off ratio of 279 and a resistance of 1.46×10^7.

Device	On/Off Ratio	Resistance	Device	On/Off Ratio	Resistance
1	1.1	9.44×10^{8}	14	12	3.08×10^{6}
2	1.1	1.86×10^{8}	15	15	2.75×10^{6}
3	1.3	2.18×10^{6}	16	20	5.89×10^{6}
4	1.4	4.73×10^{9}	17	24	8.39×10^{7}
5	2.1	3.19×10^{6}	18	40	2.70×10^{7}
6	2.1	1.45×10^{6}	19	42	1.03×10^{8}
7	2.2	9.22×10^{6}	20	43	4.94×10^{6}
8	2.6	4.12×10^{7}	21	119	5.73×10^{7}
9	4.5	1.05×10^{8}	22	188	3.64×10^{6}
10	4.5	1.97×10^{8}	23	279	1.46×10^{7}
11	5.1	2.26×10^{9}	24	649	2.30×10^{8}
12	5.9	1.85×10^{7}	25	703	1.09×10^{8}
13	8.8	3.77×10^{7}	26	1275	5.71×10^{7}

Table 3.1 Electrical results for individual devices. On/off ratios and resistances were calculated at 1 V, with the exception of devices 25 and 26. At 1 V, devices 25 and 26 produced currents too large for our test setup, so their values were calculated at 0.5 V.

Chapter 4

Discussion

In order to understand the distribution of nanotube species after isopycnic centrifugation, a simple model was constructed for the total density ρ of the nanotube-surfactant system:

$$\rho = \frac{m_n + m_s}{V_n + V_s}, \tag{4.1}$$

where m_n is the mass of the nanotube, m_s is the mass of the surfactant, V_n is the volume of the nanotube, and V_s is the volume of the surfactant. These masses and volumes can also be modeled in a simple way, as shown below.

$$m_n = 2\pi r l \sigma_g \tag{4.2}$$

$$m_s = \pi \left((r + \Delta)^2 - r^2 \right) l \rho_s \tag{4.3}$$

$$V_n = \pi r^2 l \tag{4.4}$$

$$V_s = \pi \left((r + \Delta)^2 - r^2 \right) l \tag{4.5}$$

Here, r and l are the radius and length of the nanotube, σ_g is the surface density of graphene, ρ_s is the density of the surfactant, and Δ is the constant thickness of the surfactant encapsulation layer. When these expressions are substituted into equation

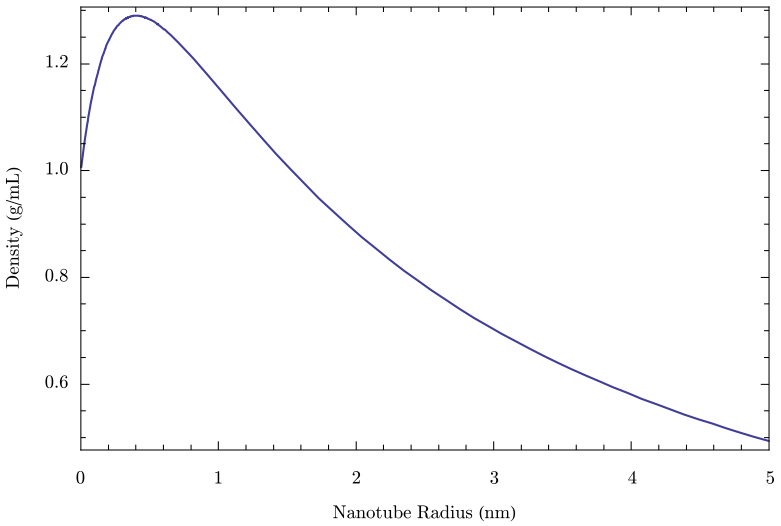

Figure 4.1 A simple model shows that the density of the nanotube-surfactant system increases with radius up to a critical point, after which it decreases with radius, as expected.

4.1, the following formula is derived:

$$\rho = \frac{\Delta(2r + \Delta)\rho_s + 2r\sigma_g}{(r + \Delta)^2}. \tag{4.6}$$

When plotted with $\sigma_g = 7.663 \times 10^{-8}$ g/cm^2, $\rho_s = 1.0$ g/mL, and $\Delta = 0.85$ nm, it becomes apparent that for small radii, density *increases* with radius up to a critical point, after which it decreases with radius, as expected (see Figure 4.1). With this value of Δ, our experimentally determined value for the density of the $(7, 6)$ fraction, which was 1.08 g/mL, is accurately predicted. This model explains the density distribution encountered in this study, since all of the species used here have radii smaller than 0.5 nm.

The narrow distribution associated with $(6, 5)$ nanotubes may suggest that this species is easier to isolate when compared to the $(7, 6)$ species. However, it is believed that higher resolution may be possible when the many parameters of isopycnic centrifugation are fully explored. For example, repeated centrifugation, though not

attempted in this study, has been shown to increase resolution.[1] Additionally, alternative density gradient shapes may have advantages over the one used here. A full exploration of these variables, along with the variables associated with dielectrophoresis, will undoubtedly result in higher resolution at the purification stage, which should produce even more impressive yields of carbon nanotube transistors.

As resolution increases, there will be many more fractions to choose from at the stage of electrical measurement. Thus, alternative methods of optical characterization, such as Raman spectroscopy, will become increasingly important. Although absorption spectroscopy is extremely useful for identifying the semiconducting species in a given sample, it is not capable of identifying metallic species. Raman spectroscopy fulfills this need. When the purification process yields larger numbers of better-resolved fractions, it will become important not only to identify the fraction with the largest population of the desired species, but also to identify the fraction with the smallest population of metallic species.

For some of the devices, source voltage sweeps resulted in asymmetric curves, with their centers severely shifted to the left or right. In some cases, this resulted in below-average on/off ratios. It is believed that this shift is due to accumulated charge on the substrate and could be prevented in a better-controlled environment. Furthermore, it is believed that the on/off ratios would be vastly improved if the contact resistance at the electrode-nanotube interface could be reduced. It is also expected that devices equipped with a direct high-κ gate, such as a hafnium top-gate, would likely perform better than those used in this study, which utilized indirect back-gates.

In conclusion, we found that isopycnic centrifugation is capable of separating $(6,5)$ species from $(7,6)$ species. We also fabricated transistors from purified $(7,6)$ nanotubes. The resultant devices displayed on/off ratios as high as 10^3 and resistances as low as 10^6, with 50% of all the devices displaying an on/off ratio greater than 10.

Although the on/off ratios of the devices in this study do not compare to those of silicon, the yields are nonetheless impressive when compared to previous studies. There is a great deal more work to be done, but this study provides a clear path for further investigation. Optimization of the processes described here may lead to an era in which the single-walled carbon nanotube becomes a viable replacement for silicon transistors.

References

[1] M.S. Arnold, A.A. Green, J.F. Hulvat, S.I. Stupp, and M.C. Hersam. Sorting carbon nanotubes by electronic structure using density differentiation. *Nature nanotechnology*, 1(1):60–65, 2006.

[2] S.M. Bachilo, L. Balzano, J.E. Herrera, F. Pompeo, D.E. Resasco, and R.B. Weisman. Narrow (n, m)-distribution of single-walled carbon nanotubes grown using a solid supported catalyst. *JOURNAL-AMERICAN CHEMICAL SOCIETY*, 125(37):11186–11187, 2003.

[3] S.M. Bachilo, M.S. Strano, C. Kittrell, R.H. Hauge, R.E. Smalley, and R.B. Weisman. Structure-assigned optical spectra of single-walled carbon nanotubes, 2002.

[4] P.J. Burke. AC performance of nanoelectronics: towards a ballistic THz nanotube transistor. *Solid State Electronics*, 48(10-11):1981–1986, 2004.

[5] W. Fu, Z. Xu, X. Bai, C. Gu, and E. Wang. Intrinsic Memory Function of Carbon Nanotube-based Ferroelectric Field-Effect Transistor. *Nano Letters*, 9(3):921–925, 2009.

[6] N. Hamada, S. Sawada, and A. Oshiyama. New one-dimensional conductors: Graphitic microtubules. *Physical Review Letters*, 68(10):1579–1581, 1992.

[7] MC Hersam. Progress towards monodisperse single-walled carbon nanotubes. *Nature nanotechnology*, 3(7):387, 2008.

[8] R. Krupke, F. Hennrich, M.M. Kappes, and H. Lohneysen. Surface conductance induced dielectrophoresis of semiconducting single-walled carbon nanotubes. *Nano Letters*, 4(8):1395–1400, 2004.

[9] S. Reich, C. Thomsen, and J. Maultzsch. *Carbon nanotubes: basic concepts and physical properties*. Vch Verlagsgesellschaft Mbh, 2004.

[10] R. Saito, G. Dresselhaus, and MS Dresselhaus. Trigonal warping effect of carbon nanotubes. *Physical Review B*, 61(4):2981–2990, 2000.

[11] R. G. A. Veiga and David Tomanek. TubeVBS, 2007.

[12] Wolfram Research, Inc. Mathematica, Version 6.0. Champaign, IL, 2007.

Appendix A

Absorption Data

This appendix contains the absorption data referred to in this study. Fractions were taken from low to high densities and labeled sequentially. The high-frequency shift, which becomes quite prominent in the last few fractions, is caused by scattering from nanotube aggregates.

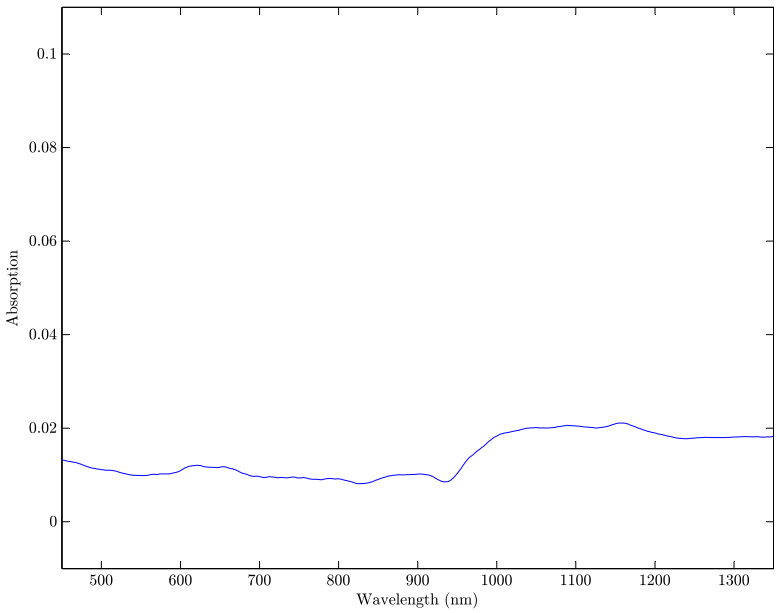

Figure A.1 Fraction 3.

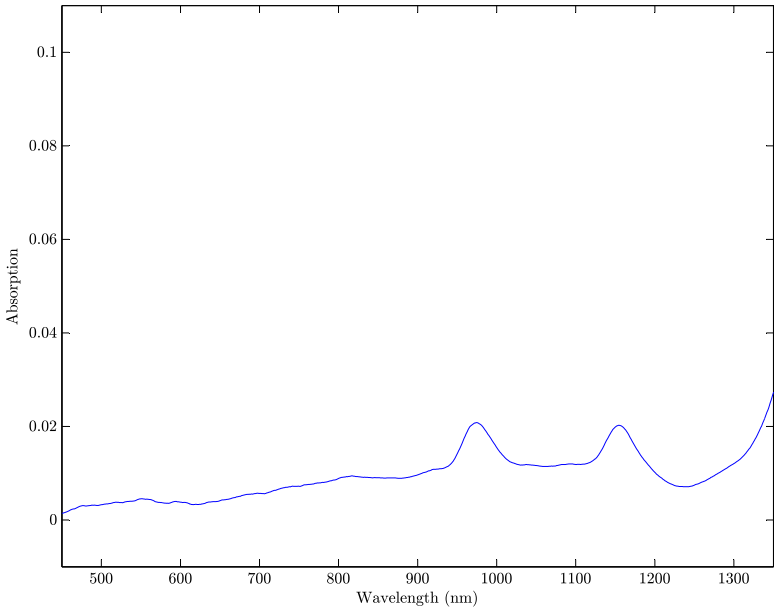

Figure A.2 Fraction 4.

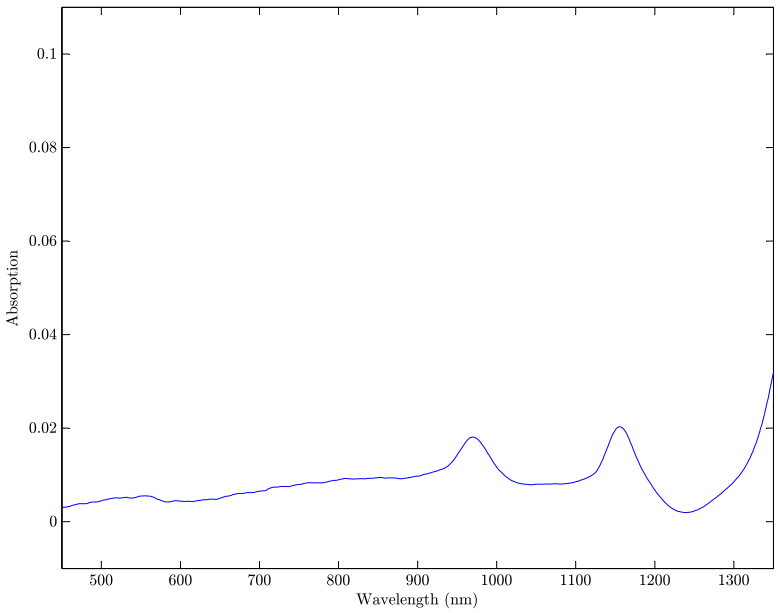

Figure A.3 Fraction 5.

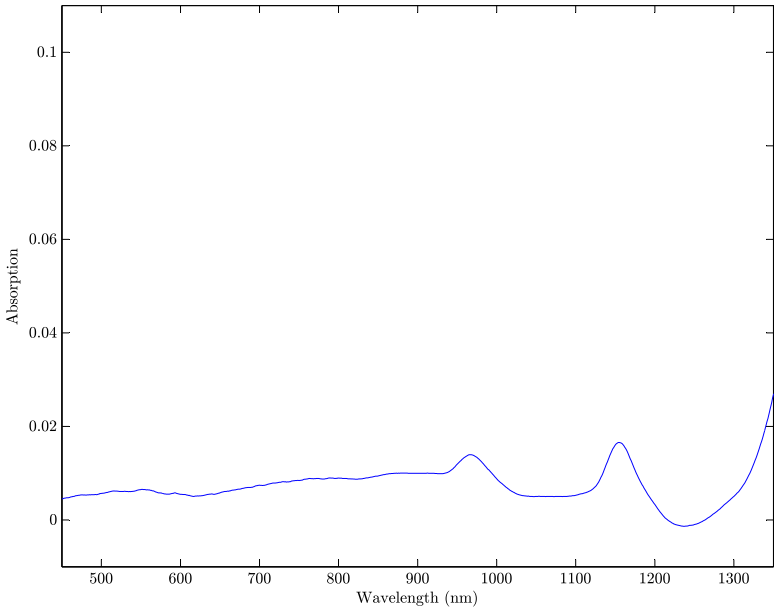

Figure A.4 Fraction 6.

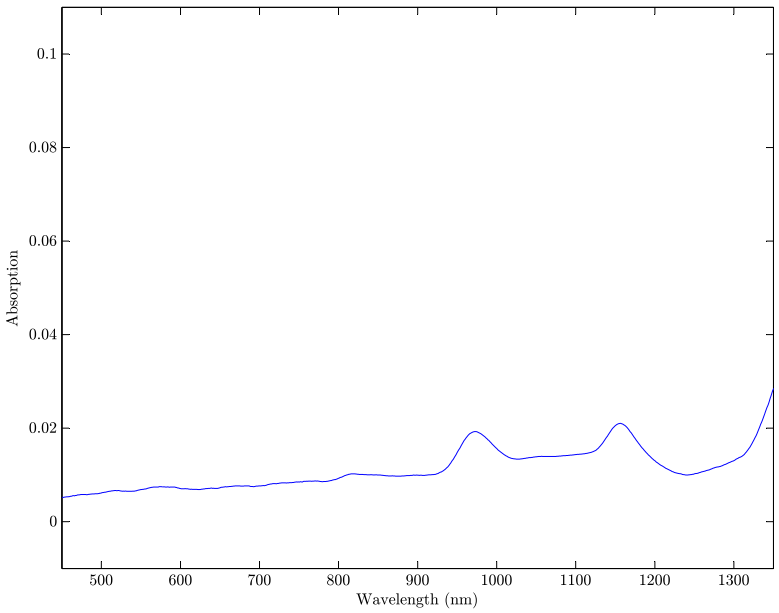

Figure A.5 Fraction 7.

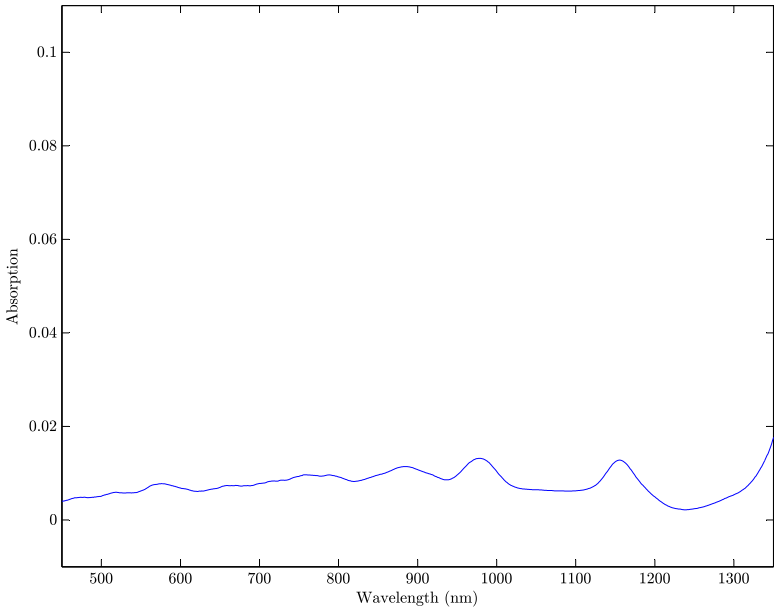

Figure A.6 Device 8.

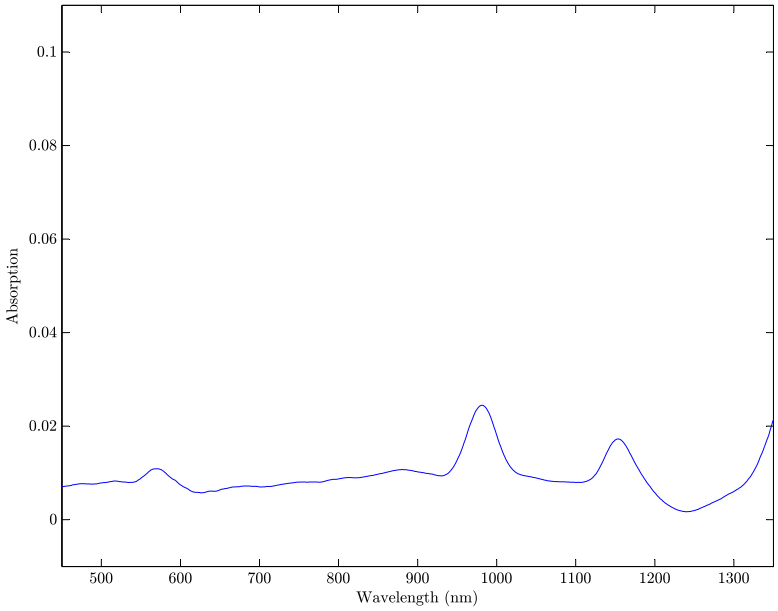

Figure A.7 Device 9.

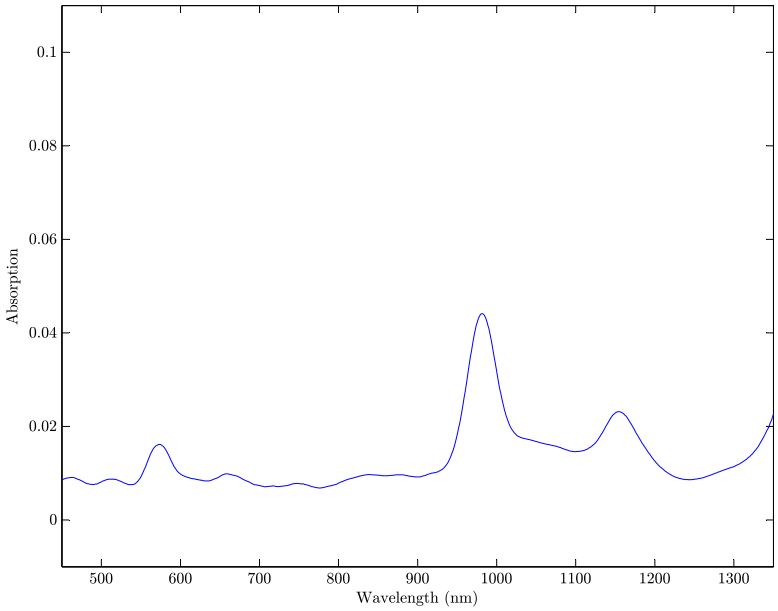

Figure A.8 Device 10.

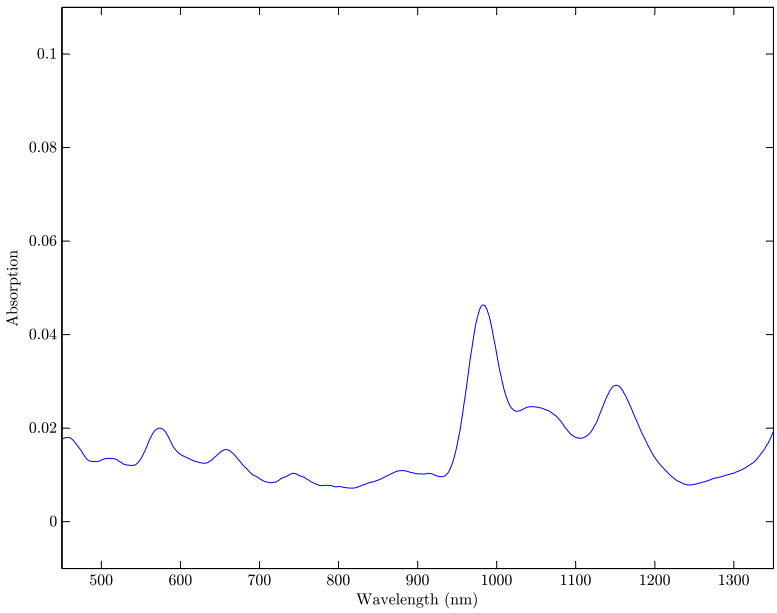

Figure A.9 Device 11.

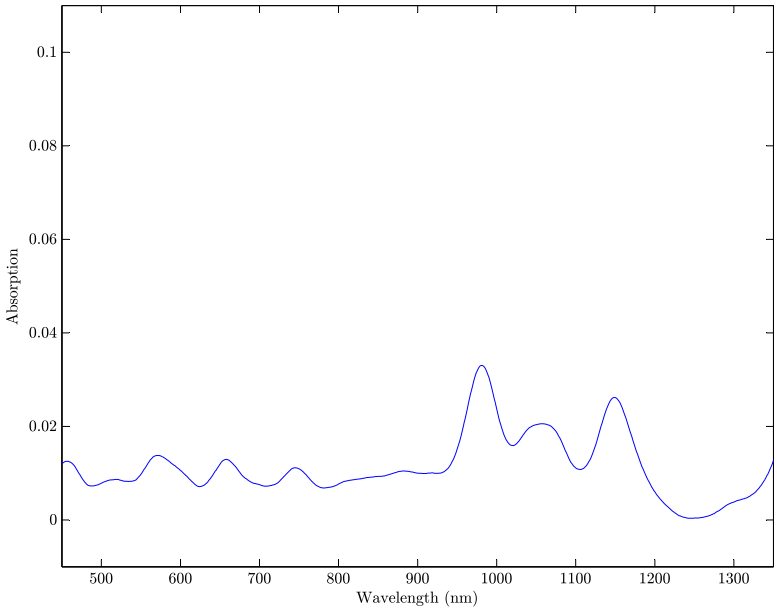

Figure A.10 Device 12.

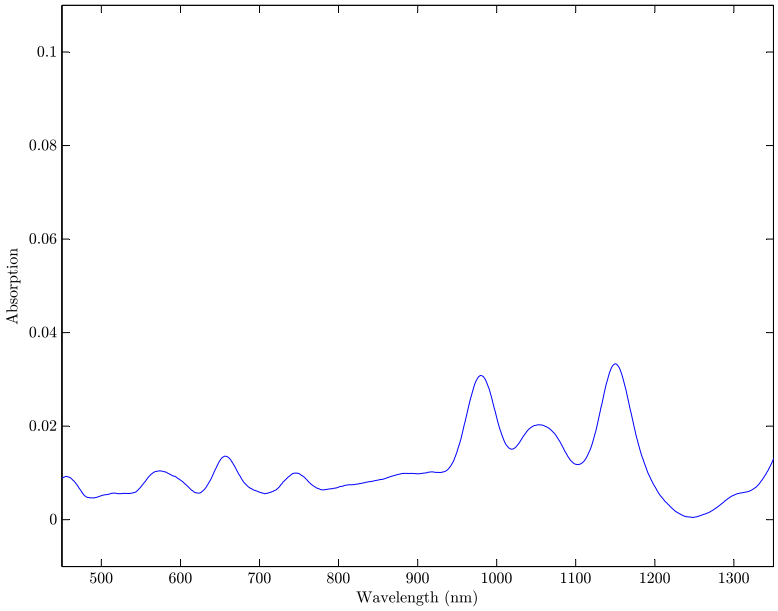

Figure A.11 Device 13.

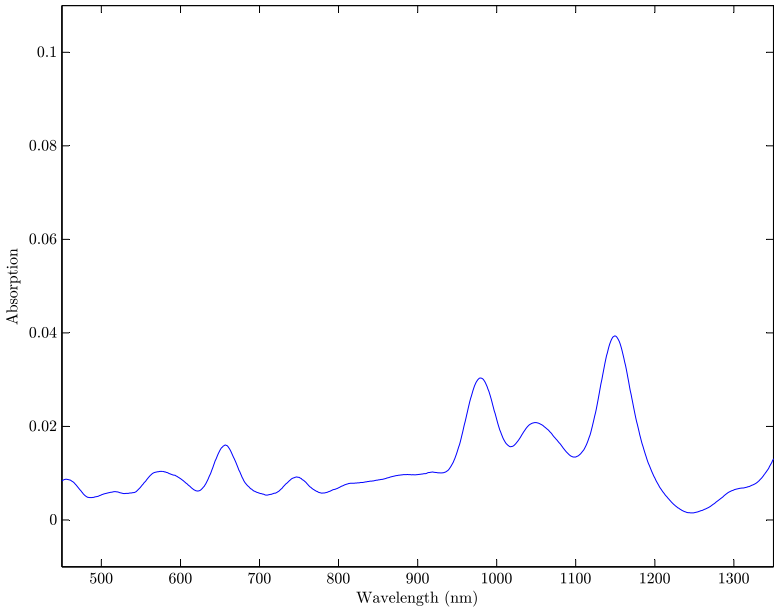

Figure A.12 Device 14.

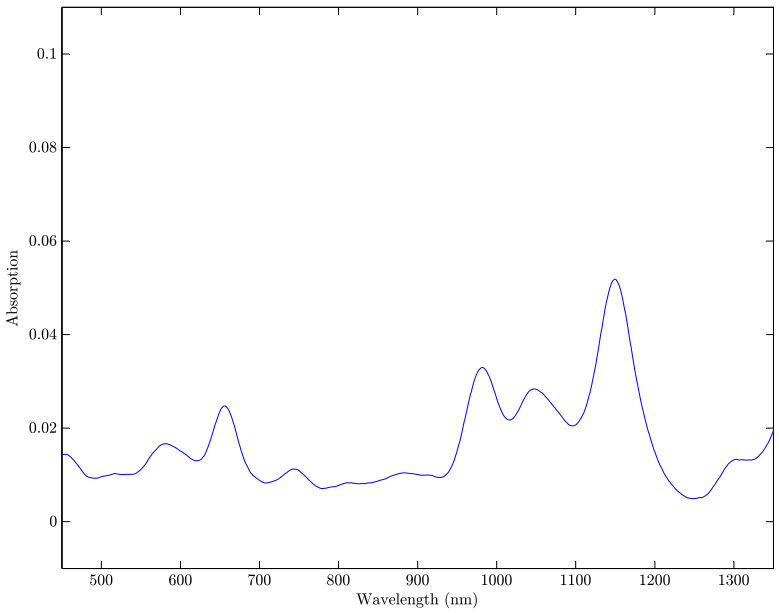

Figure A.13 Device 15.

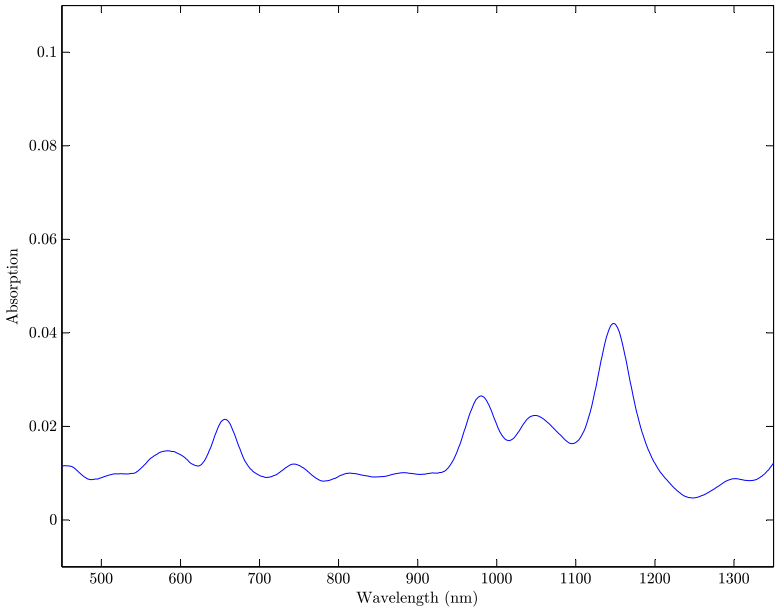

Figure A.14 Device 16.

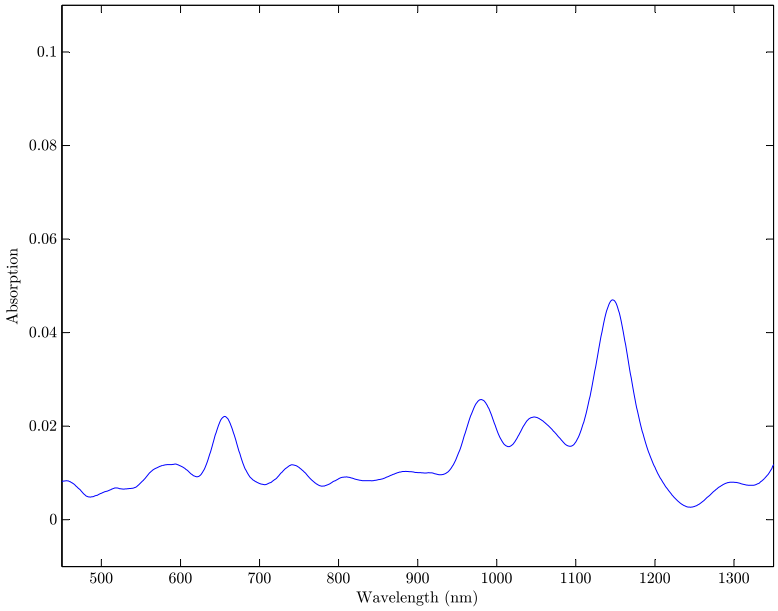

Figure A.15 Device 17.

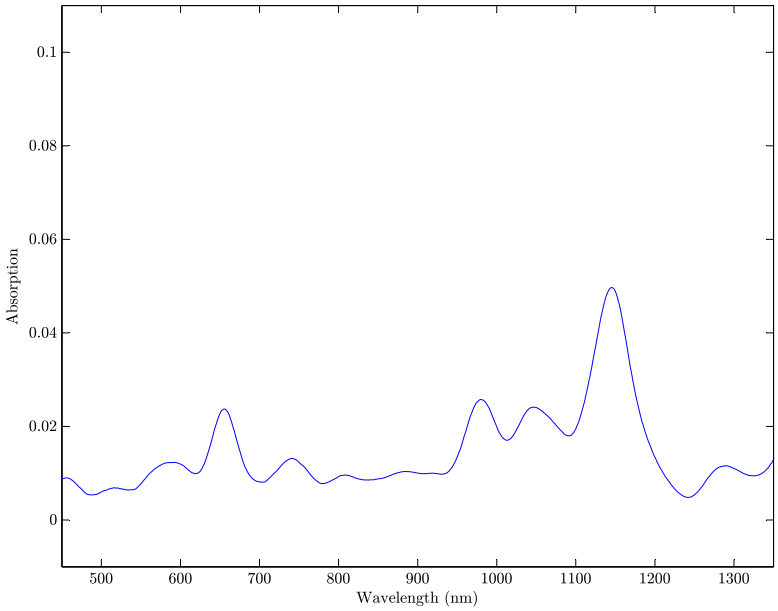

Figure A.16 Device 18.

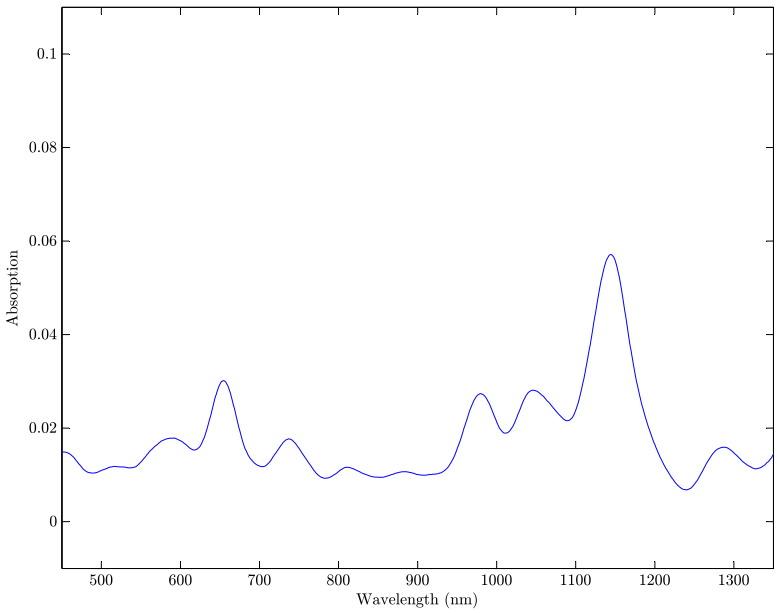

Figure A.17 Device 19.

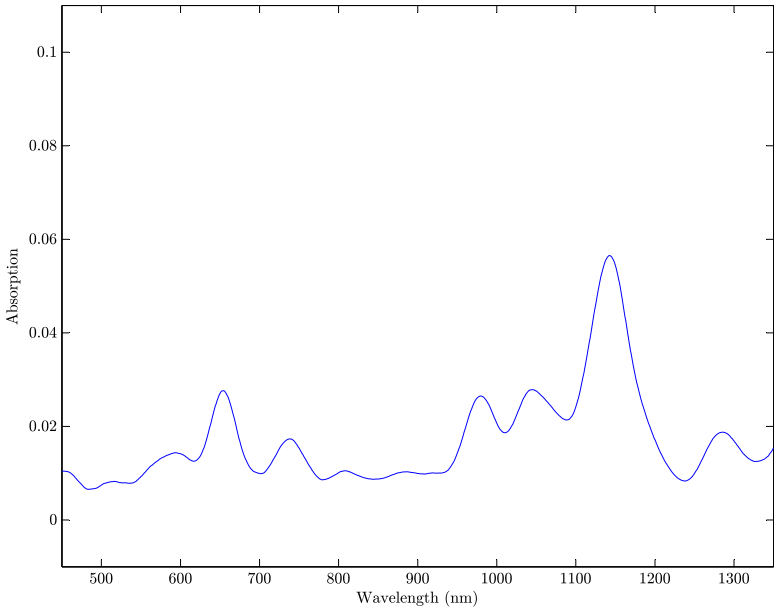

Figure A.18 Device 20.

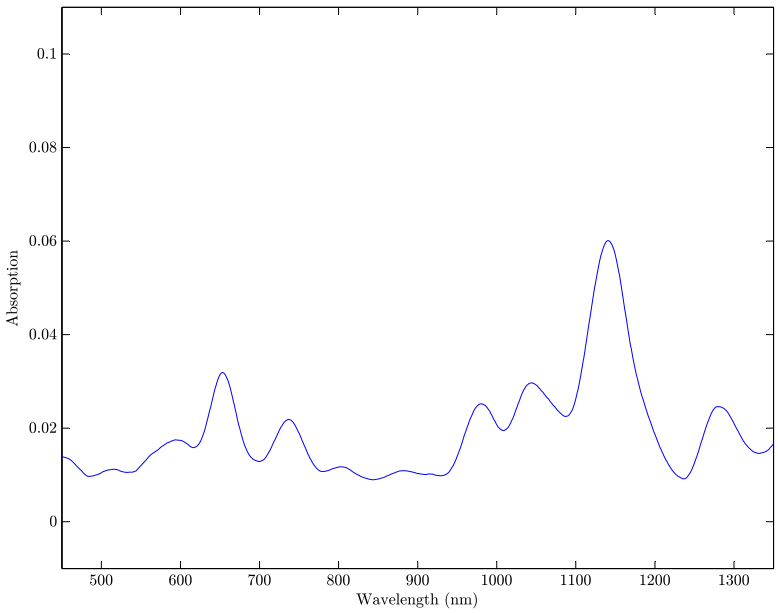

Figure A.19 Device 21.

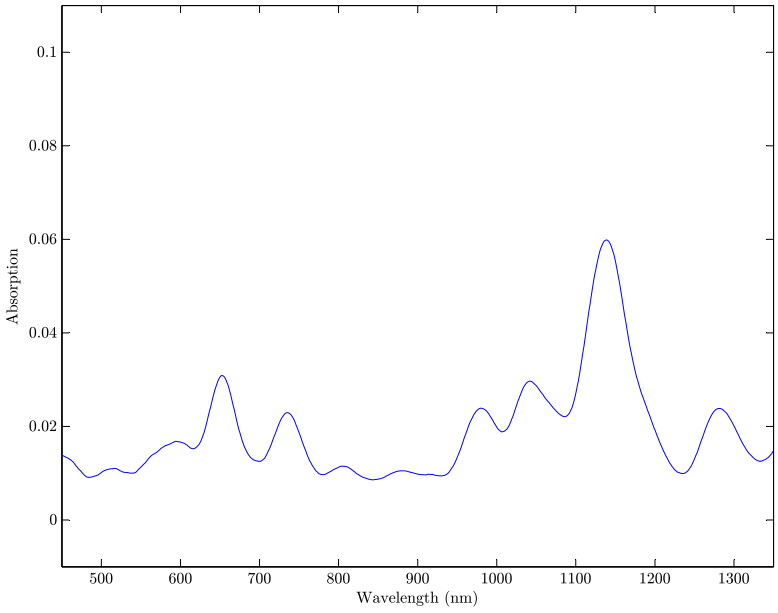

Figure A.20 Device 22.

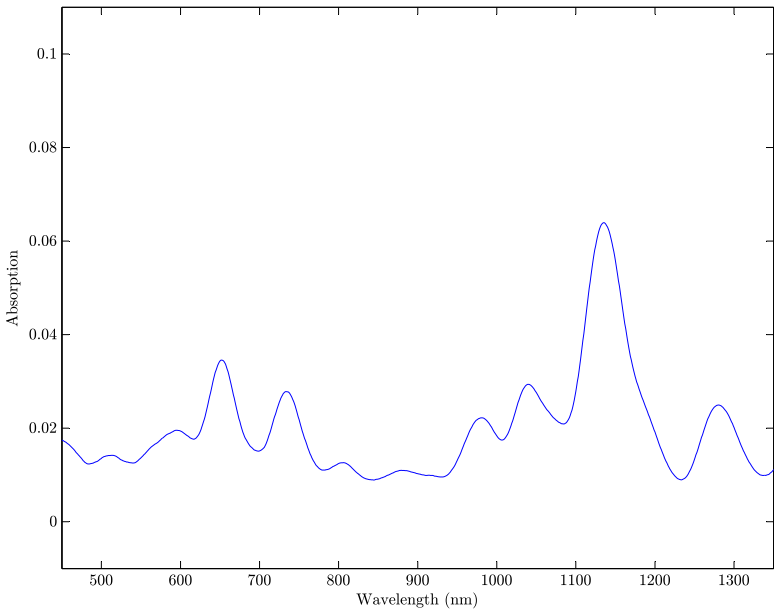

Figure A.21 Device 23.

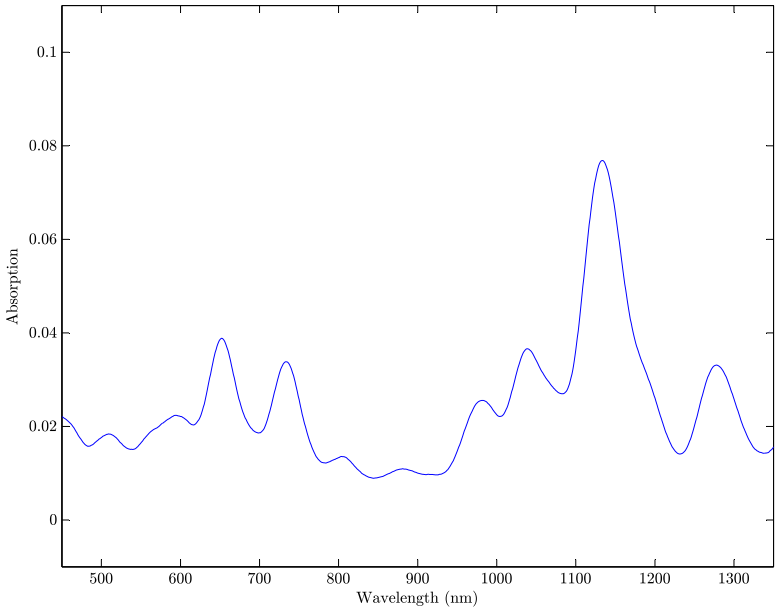

Figure A.22 Device 24.

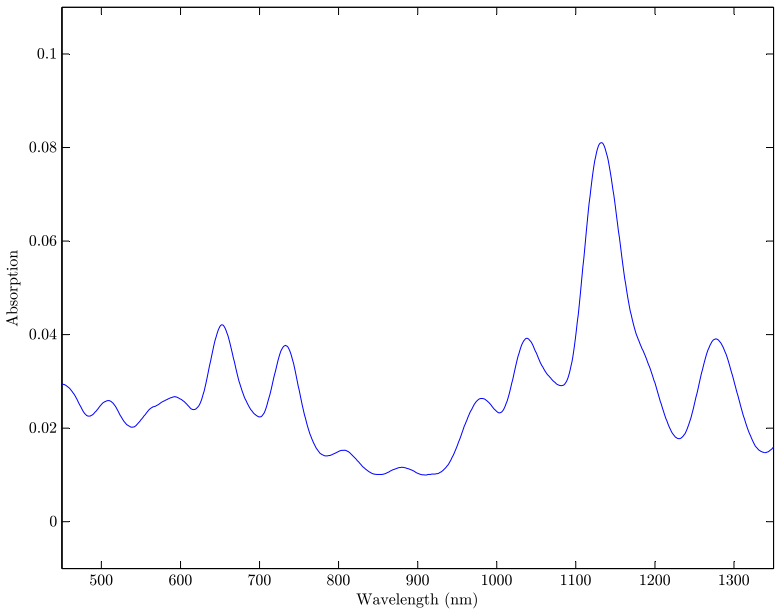

Figure A.23 Device 25.

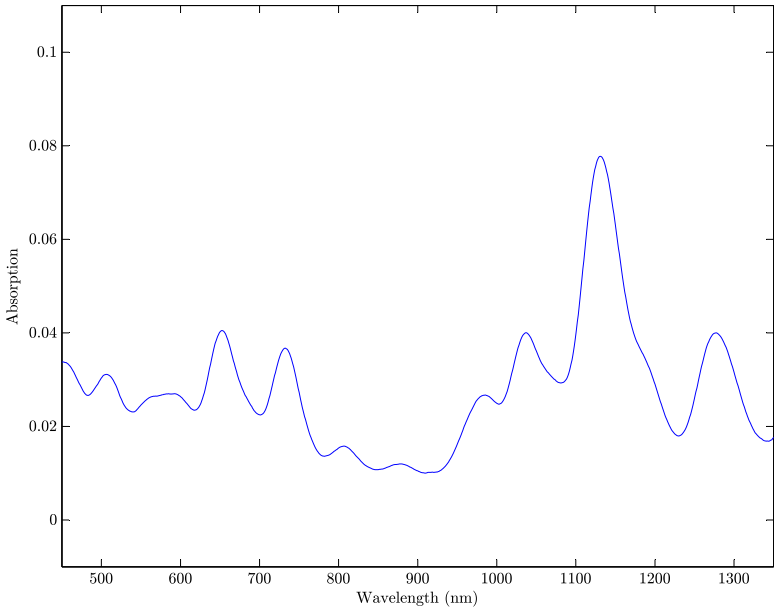

Figure A.24 Device 26.

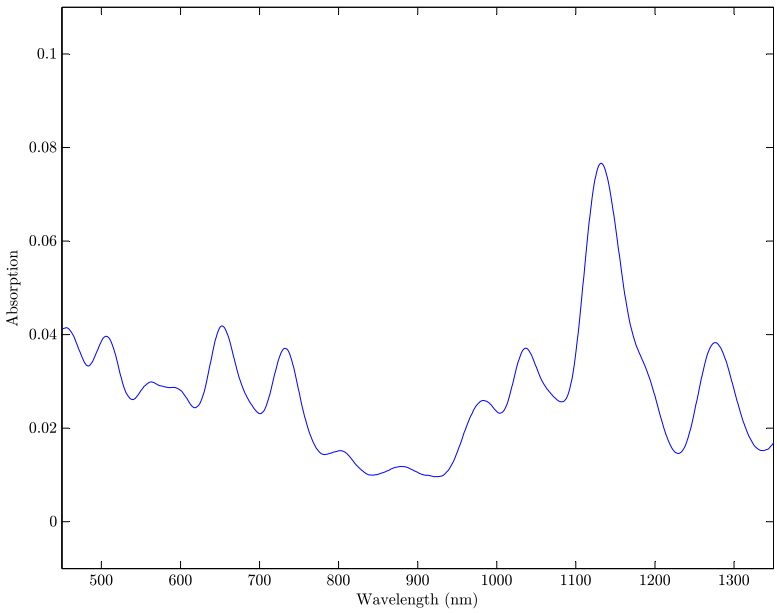

Figure A.25 Device 27.

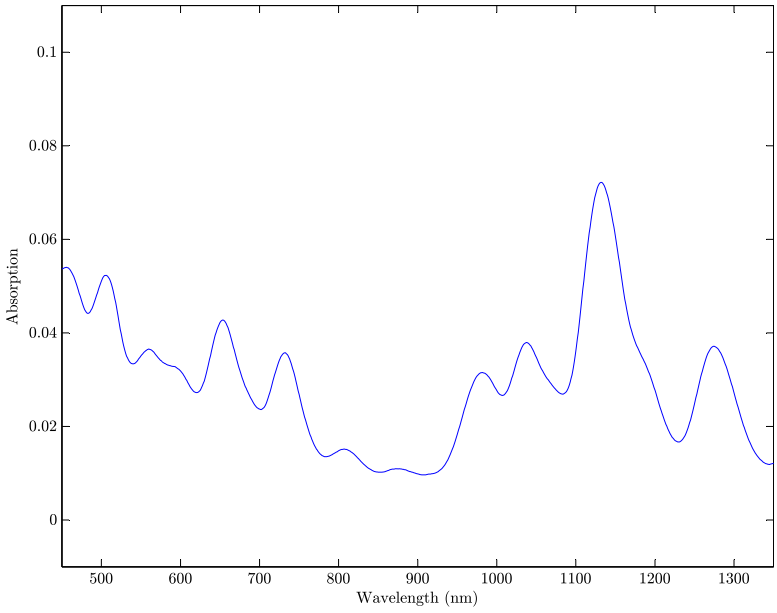

Figure A.26 Device 28.

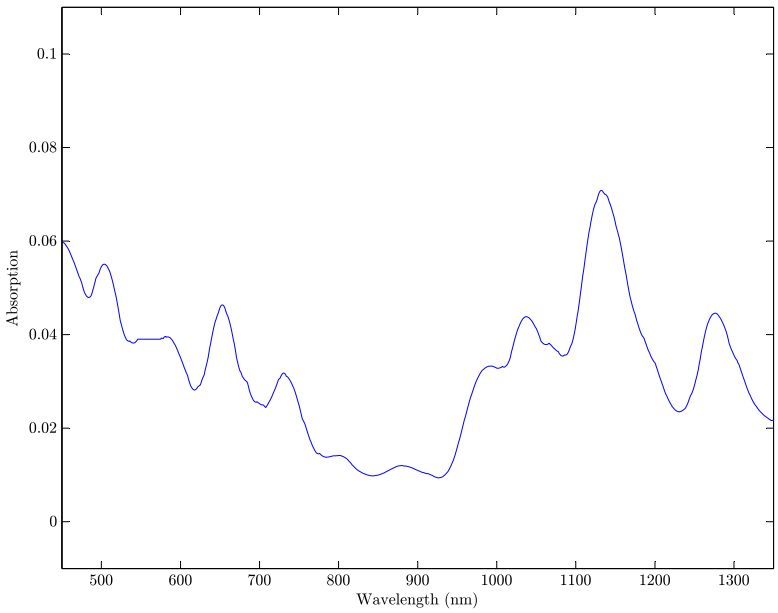

Figure A.27 Device 29.

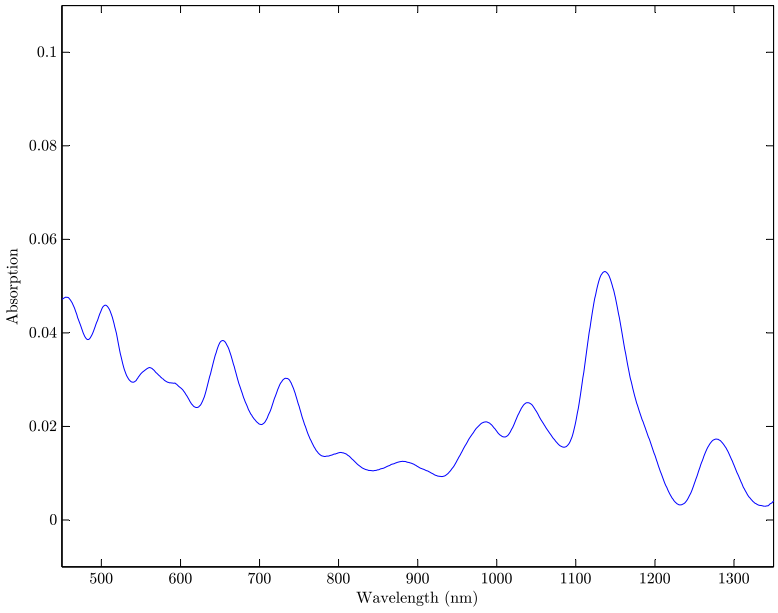

Figure A.28 Device 30.

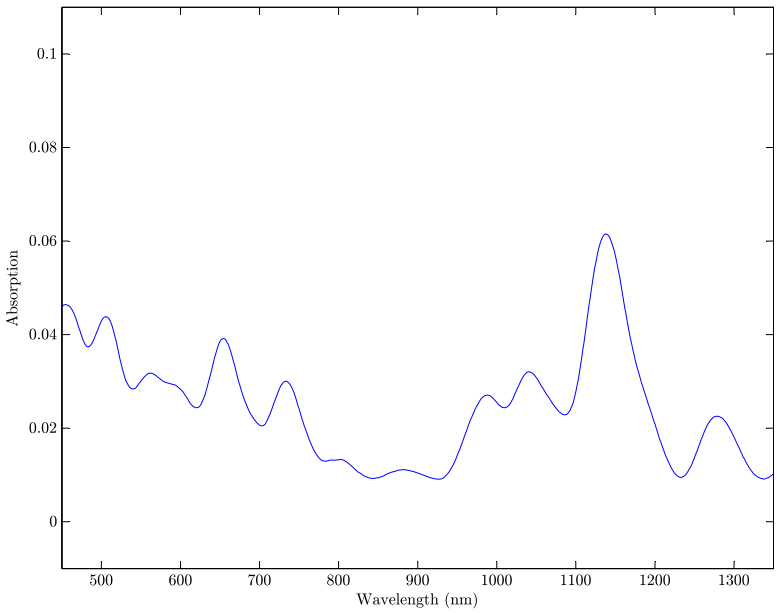

Figure A.29 Device 31.

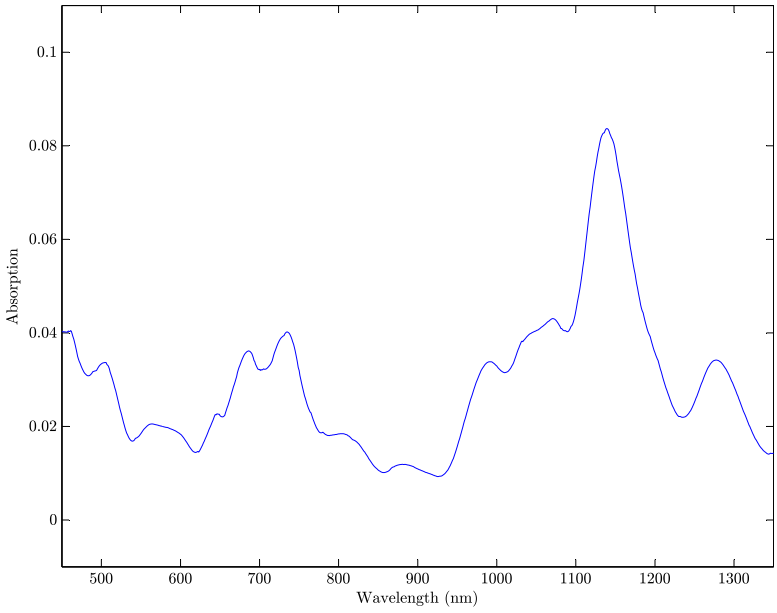

Figure A.30 Device 32.

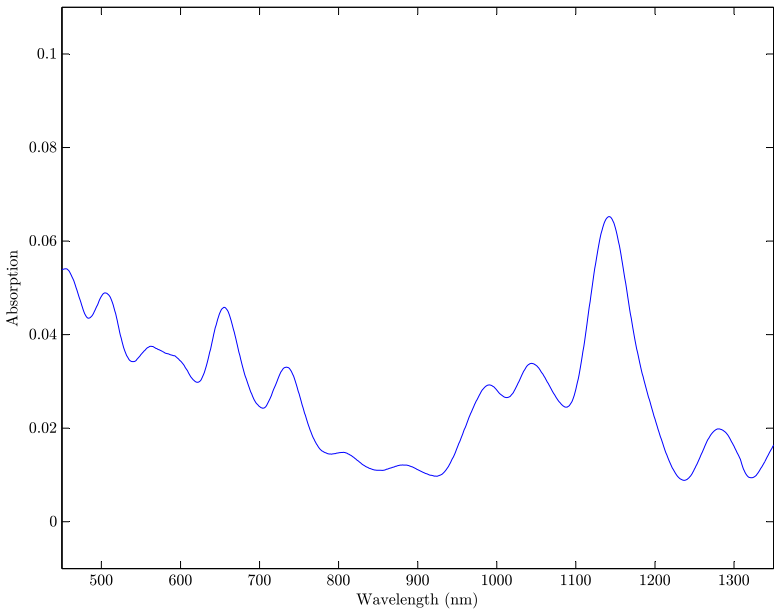

Figure A.31 Device 33.

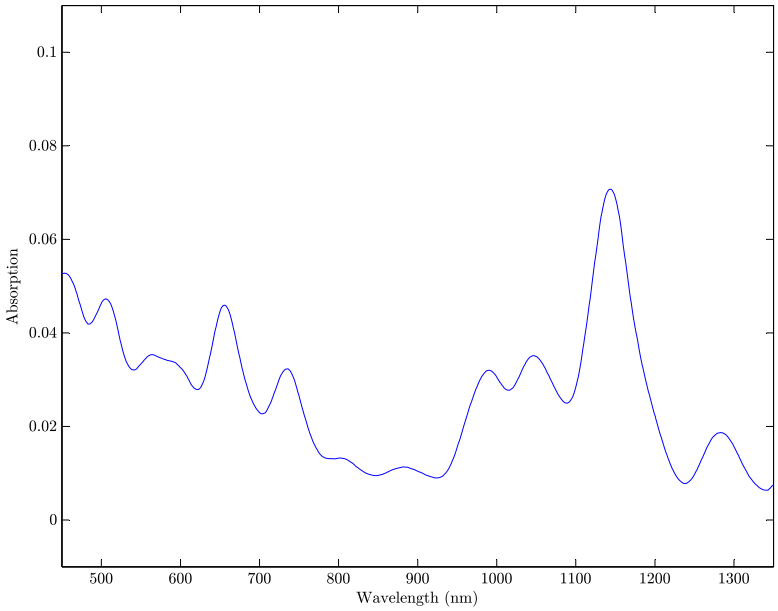

Figure A.32 Device 34.

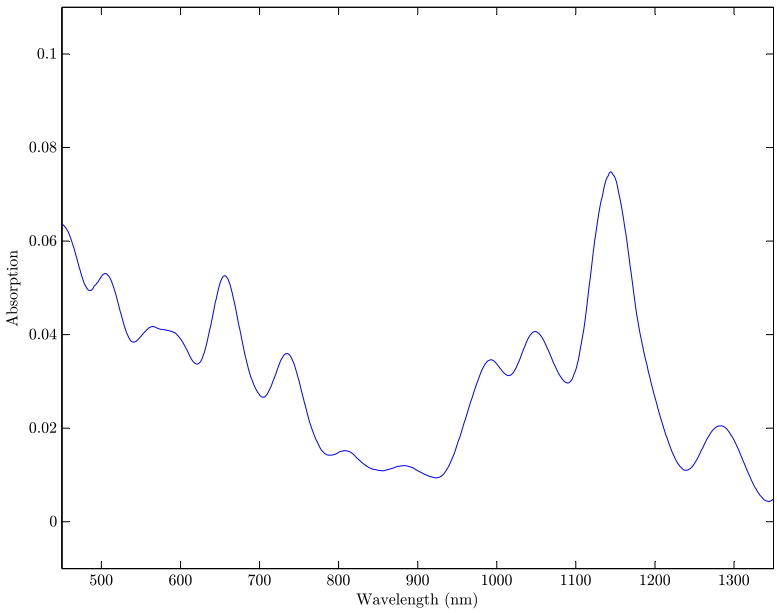

Figure A.33 Device 35.

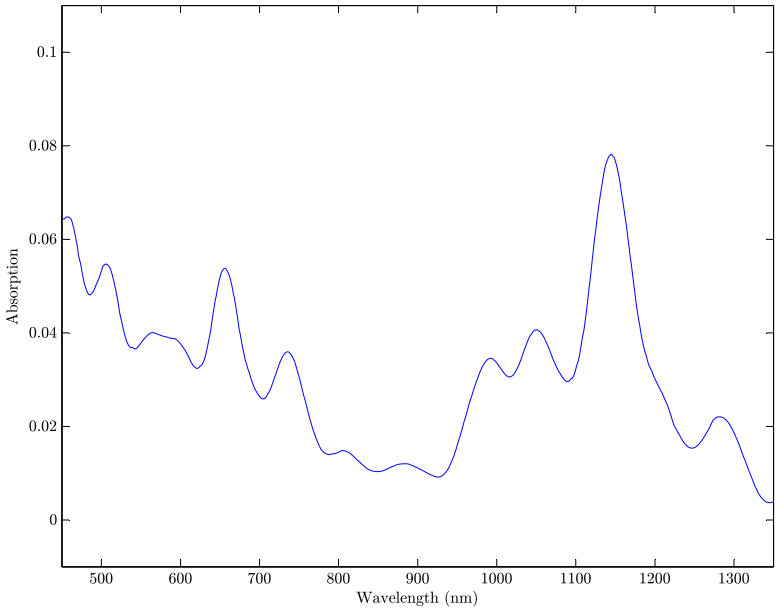

Figure A.34 Device 36.

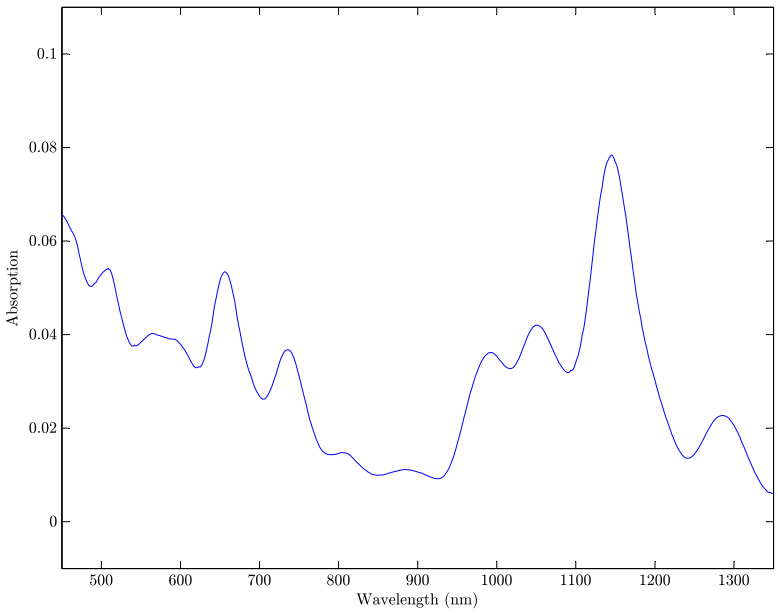

Figure A.35 Device 37.

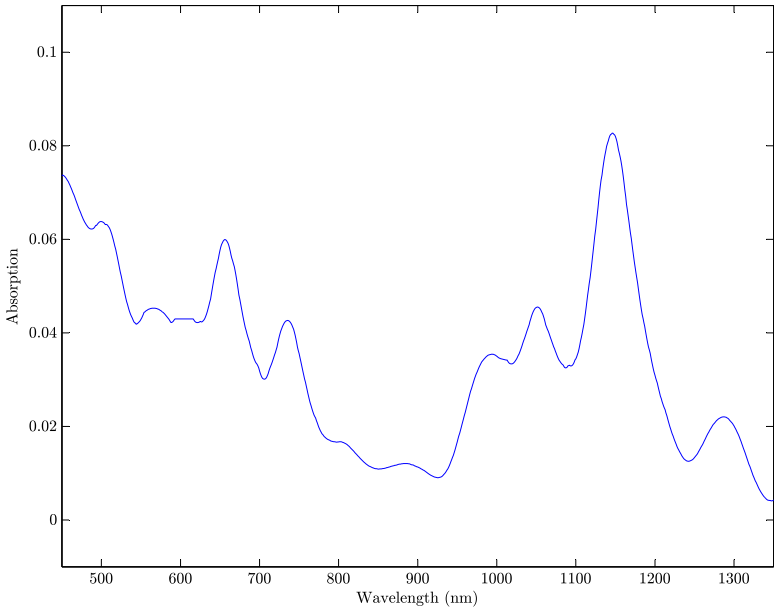

Figure A.36 Device 38.

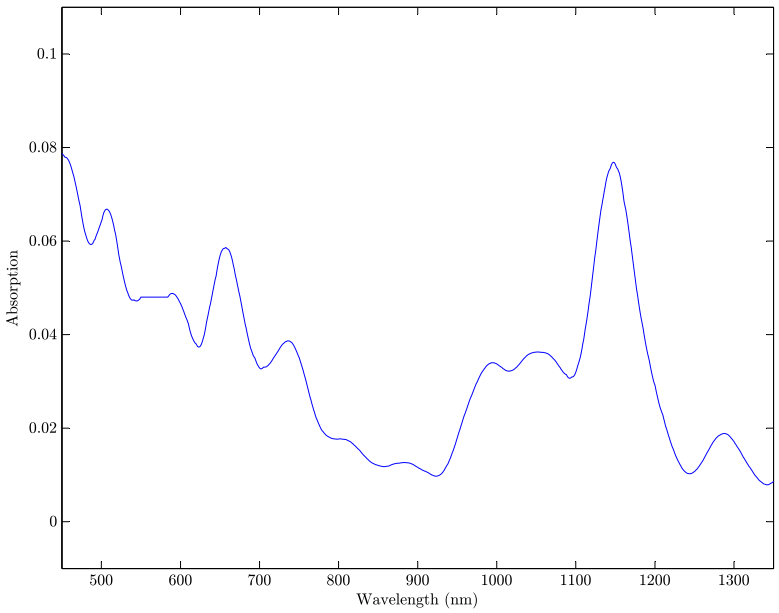

Figure A.37 Device 39.

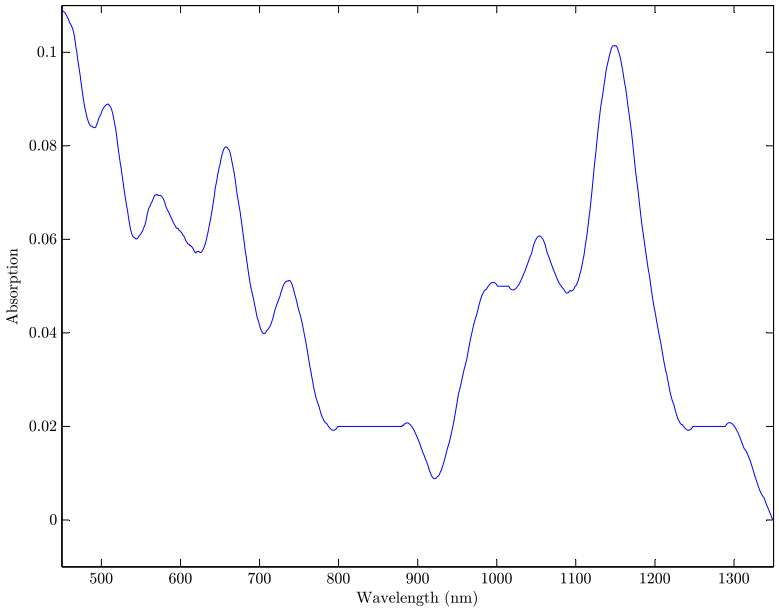

Figure A.38 Device 40.

Appendix B

Source Voltage Sweep Data

This appendix contains the source voltage sweep data referred to in this study. The source voltage was generally varied from -1 V to 1 V with gate voltages of -4 V, 0 V, and 4 V.

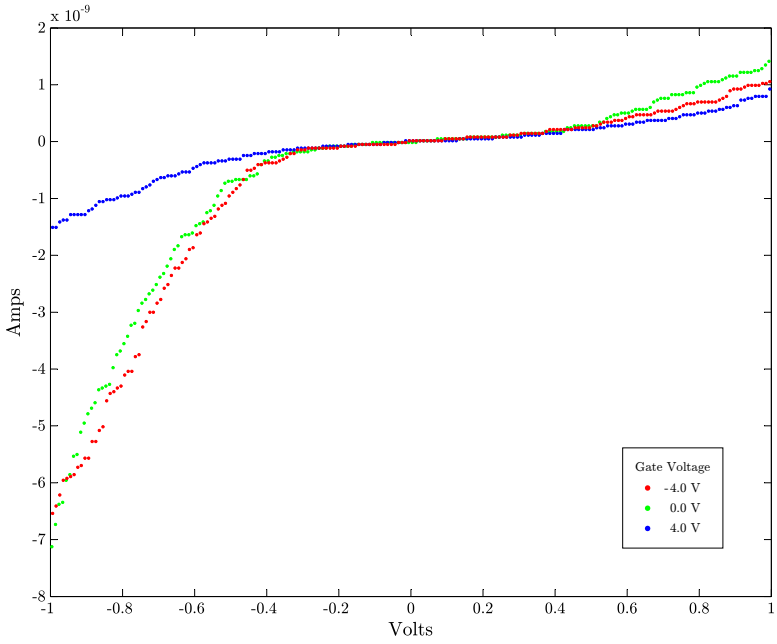

Figure B.1 Device 1.

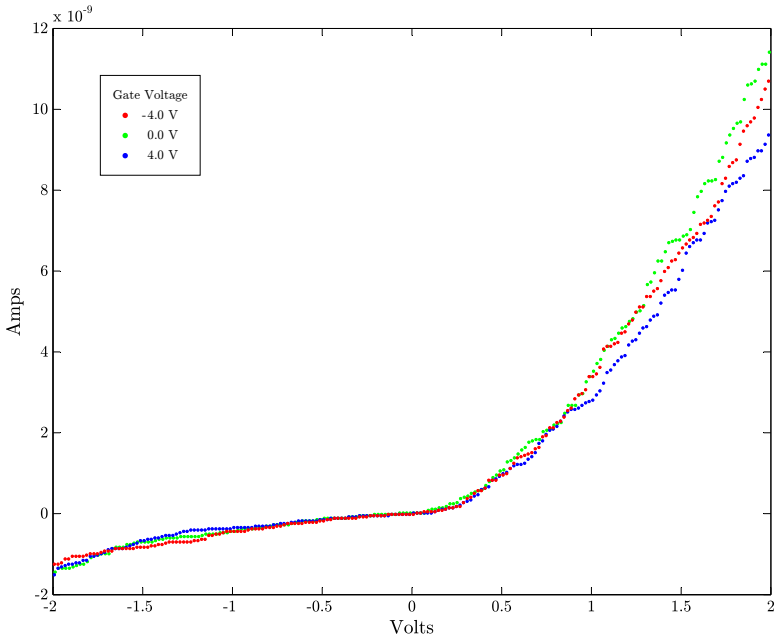

Figure B.2 Device 2.

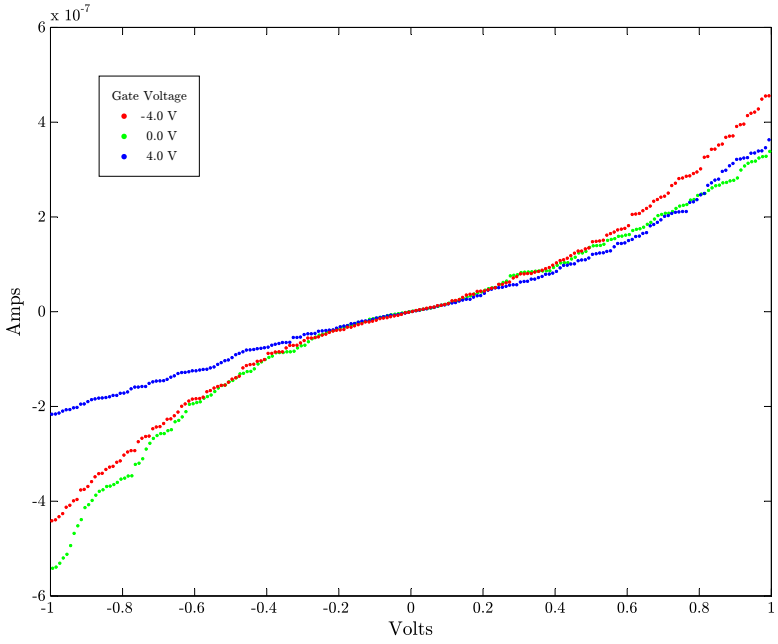

Figure B.3 Device 3.

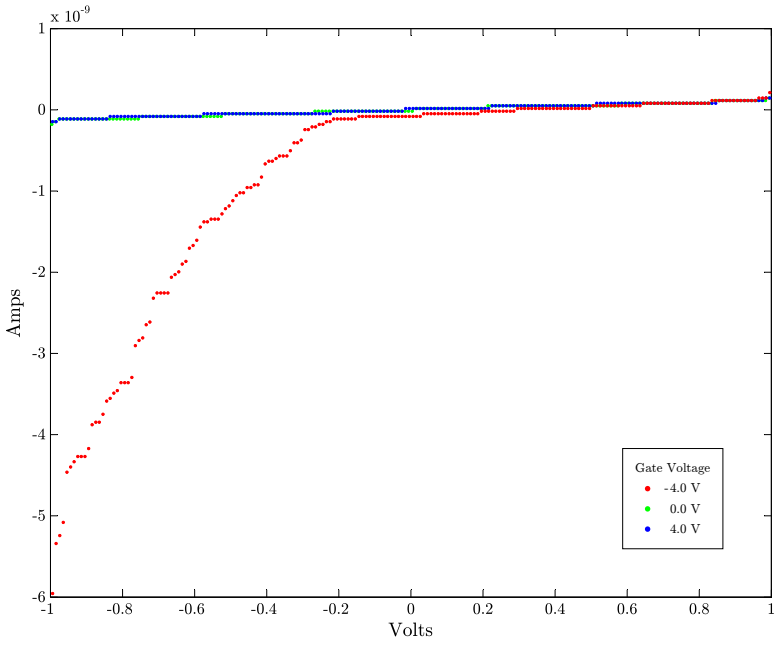

Figure B.4 Device 4.

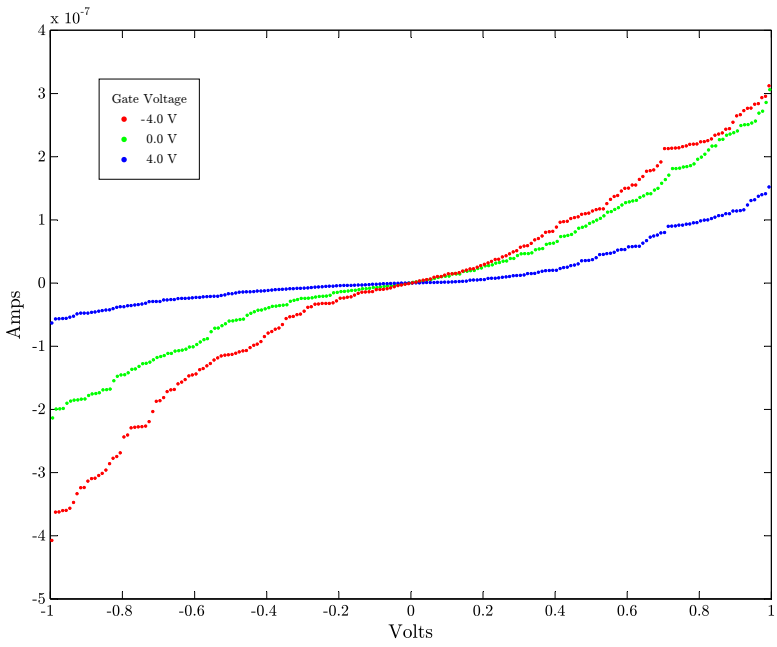

Figure B.5 Device 5.

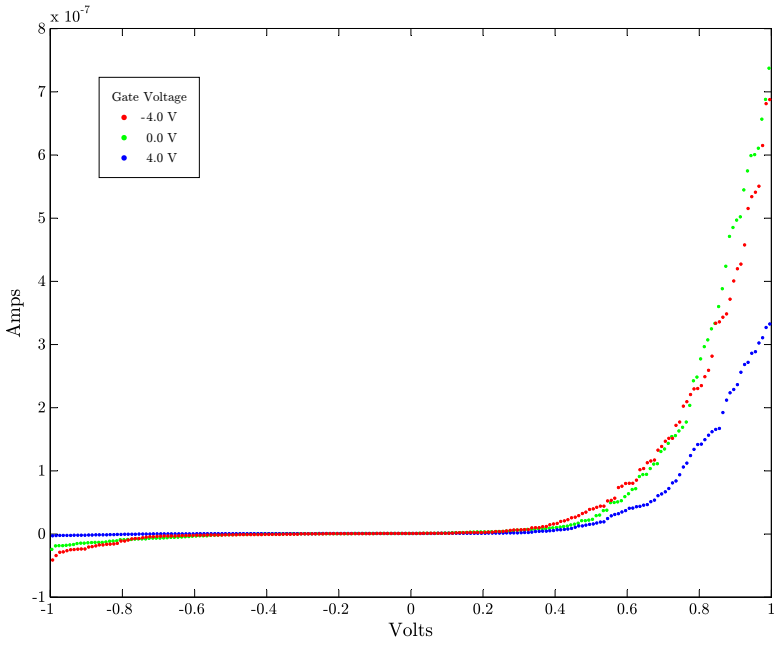

Figure B.6 Device 6.

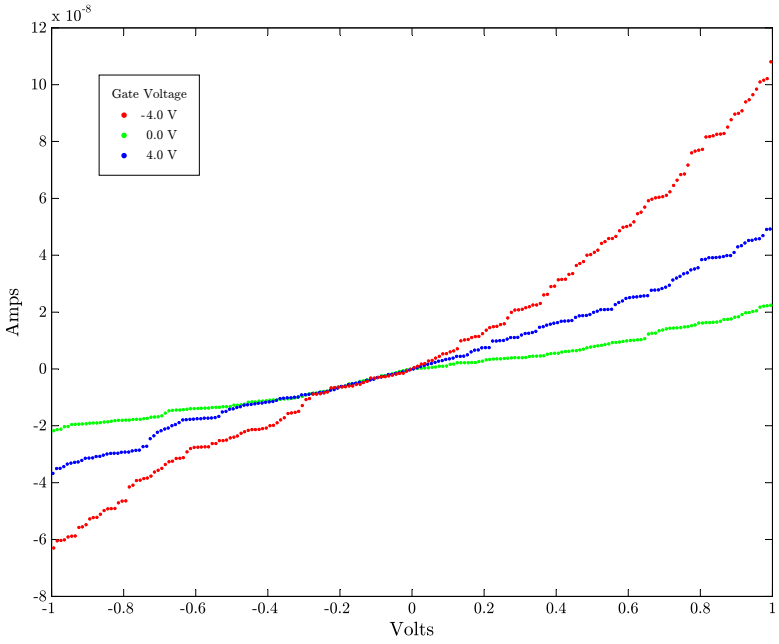

Figure B.7 Device 7.

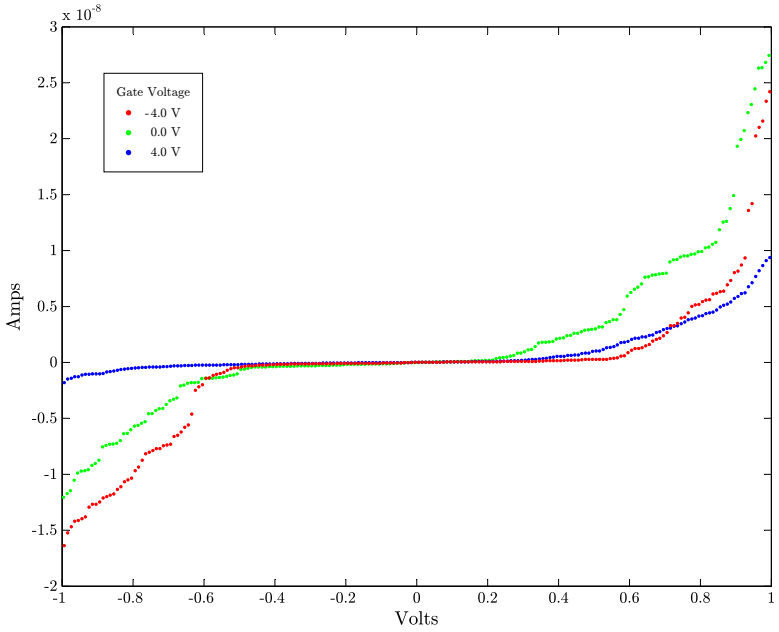

Figure B.8 Device 8.

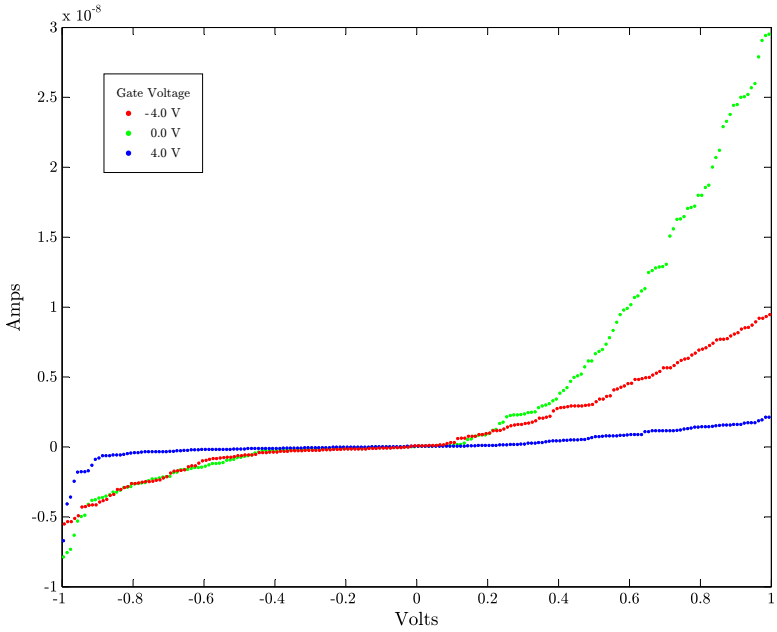

Figure B.9 Device 9.

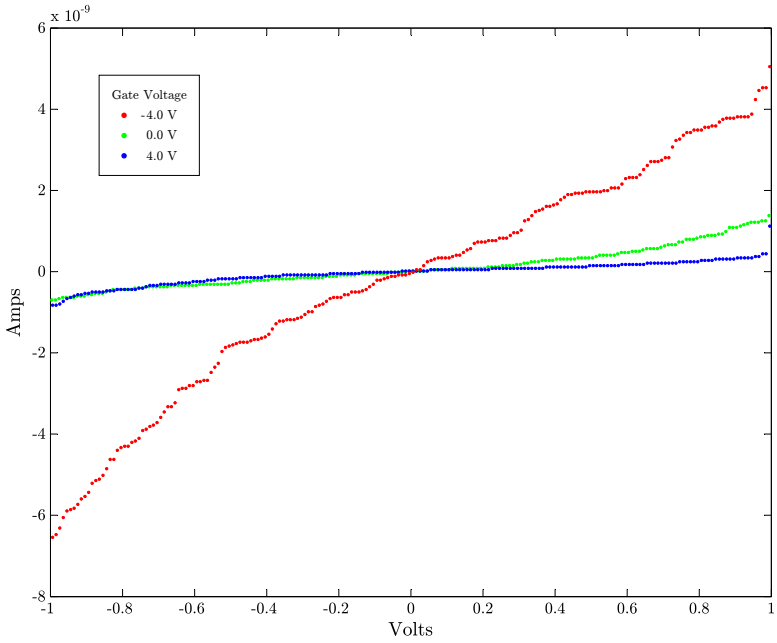

Figure B.10 Device 10.

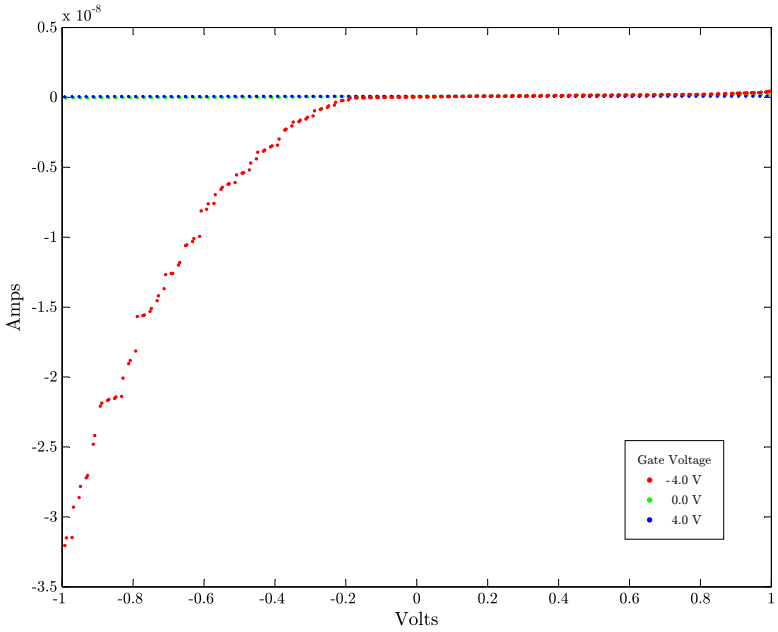

Figure B.11 Device 11.

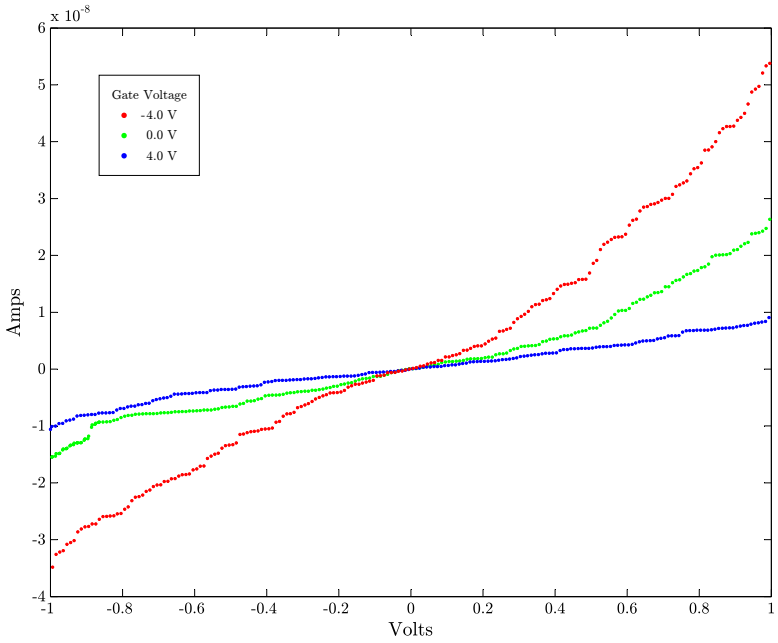

Figure B.12 Device 12.

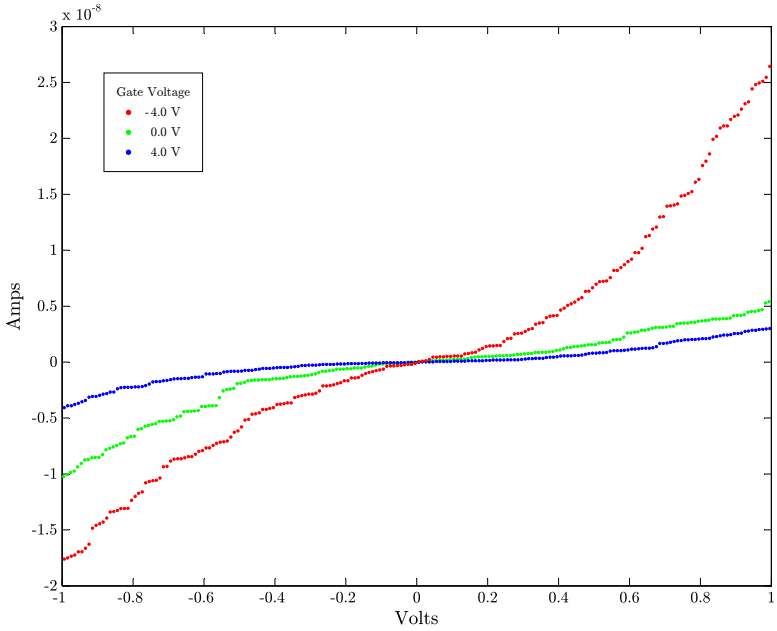

Figure B.13 Device 13.

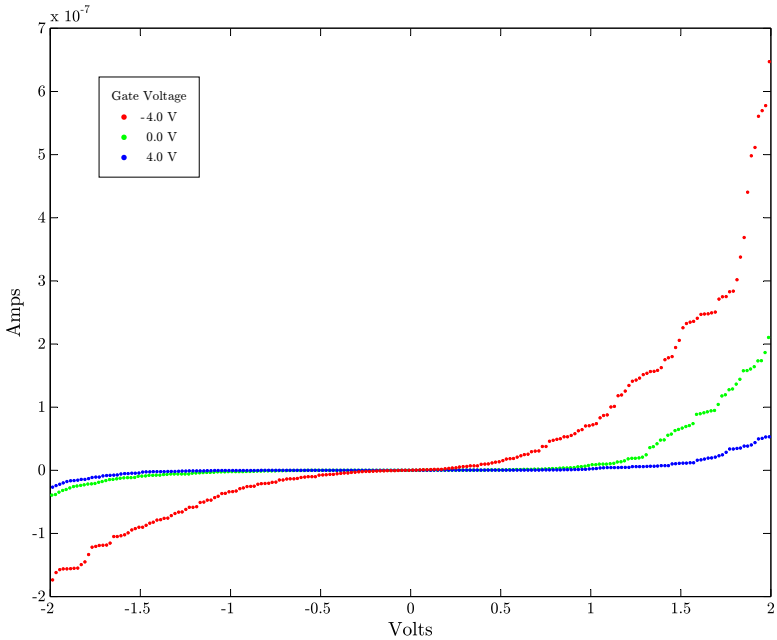

Figure B.14 Device 14.

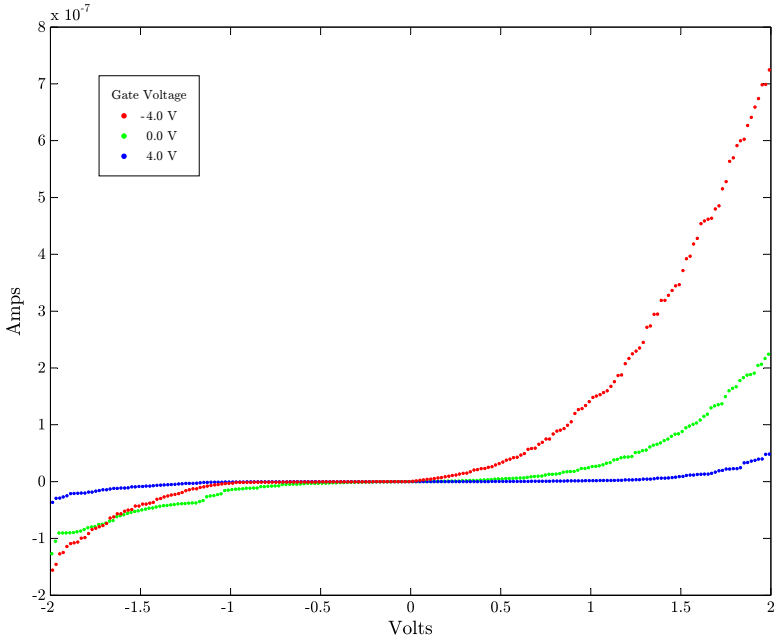

Figure B.15 Device 15.

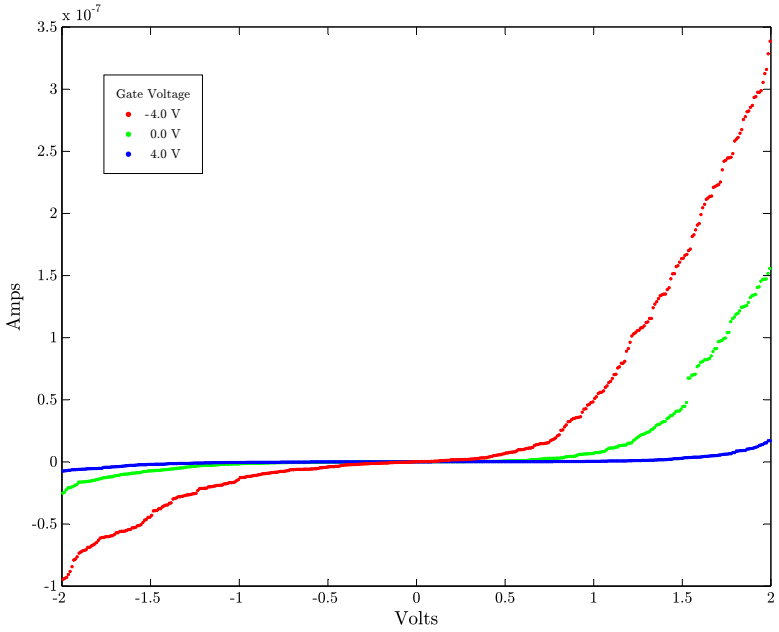

Figure B.16 Device 16.

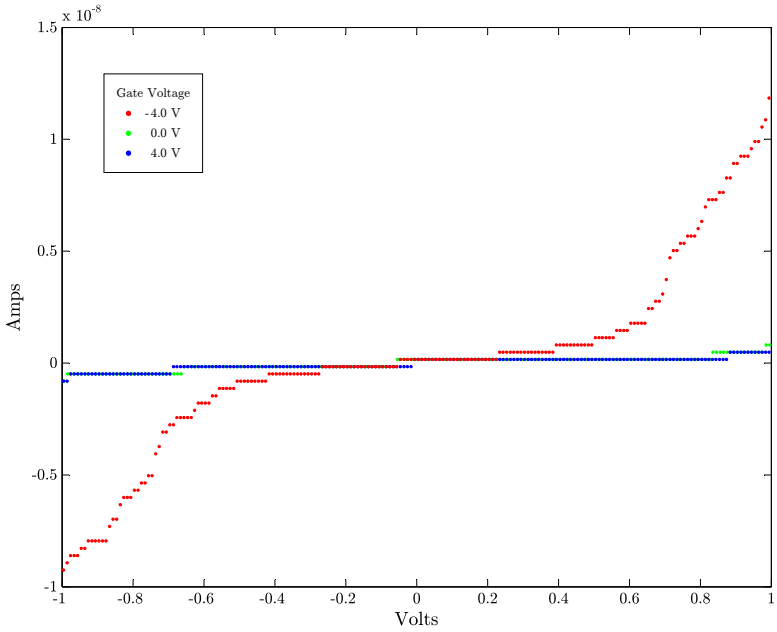

Figure B.17 Device 17.

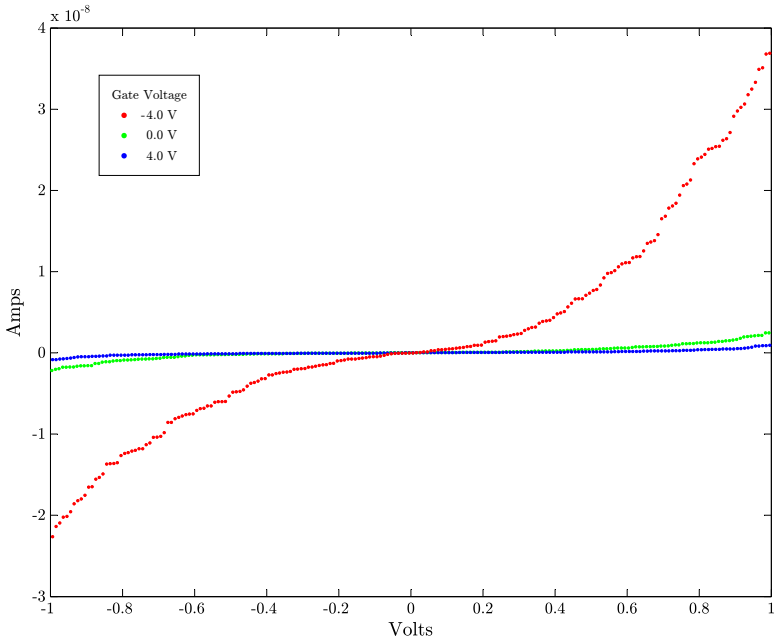

Figure B.18 Device 18.

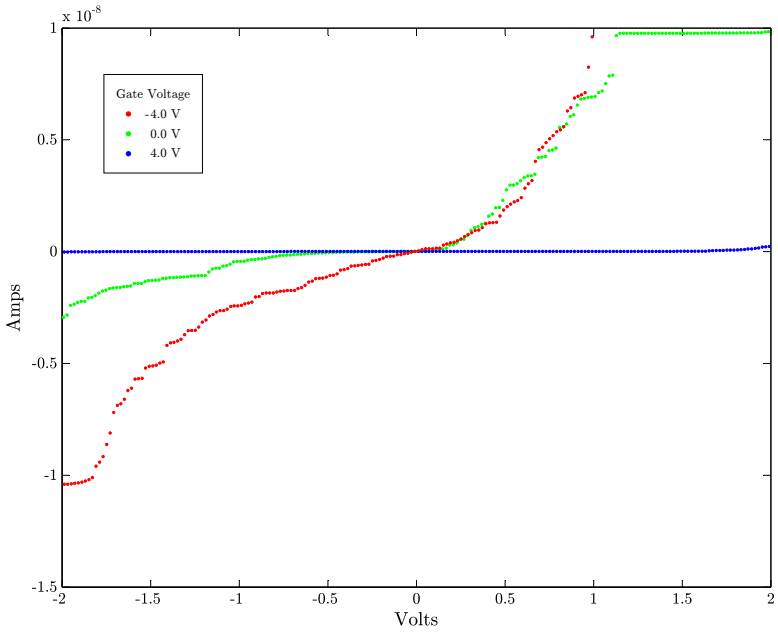

Figure B.19 Device 19.

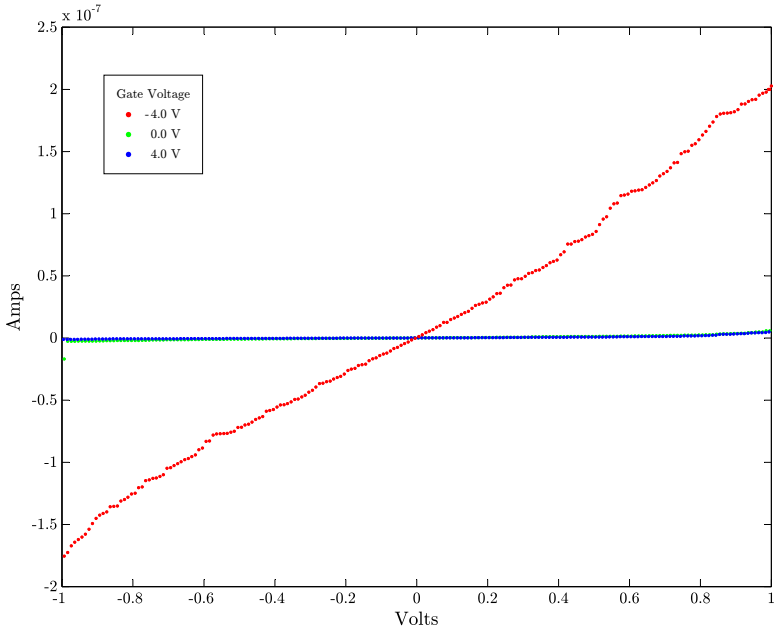

Figure B.20 Device 20.

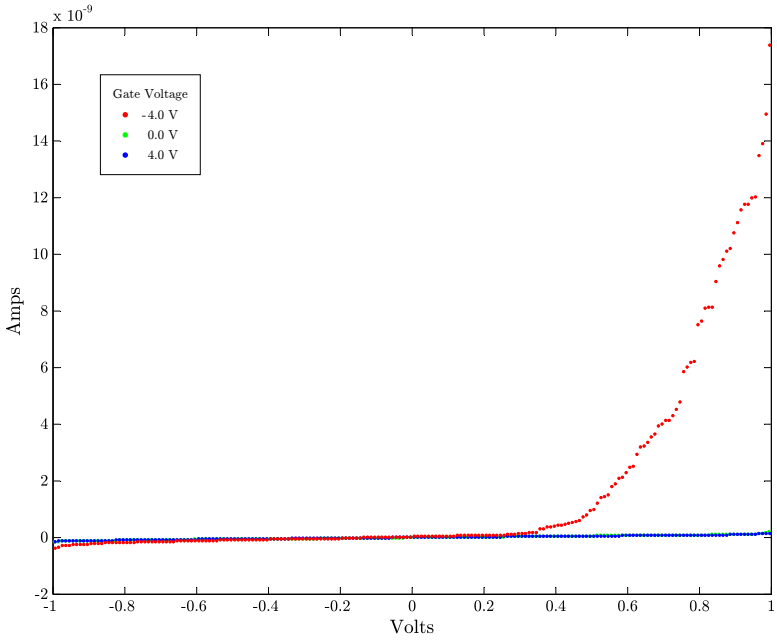

Figure B.21 Device 21.

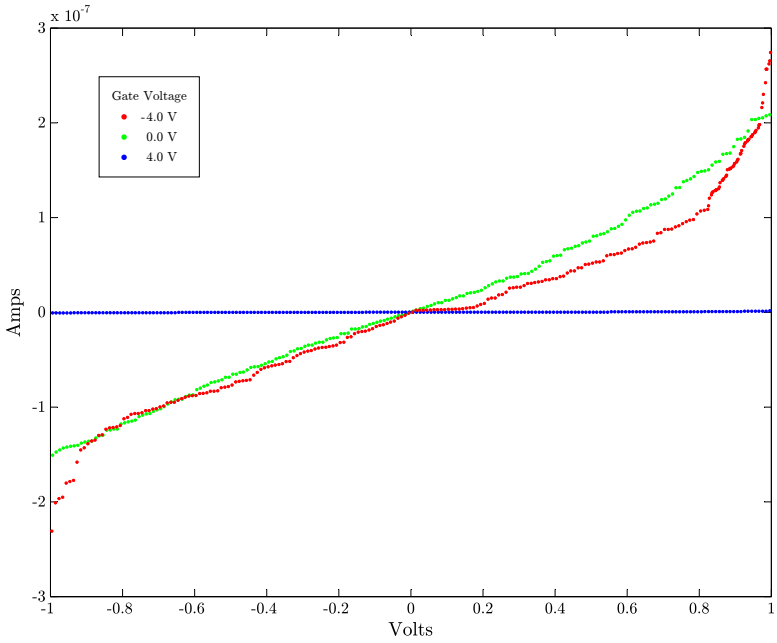

Figure B.22 Device 22.

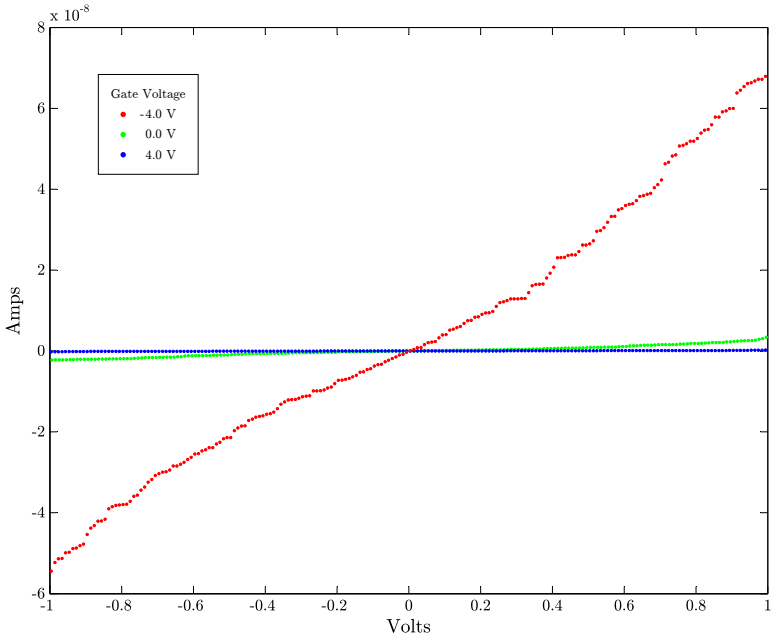

Figure B.23 Device 23.

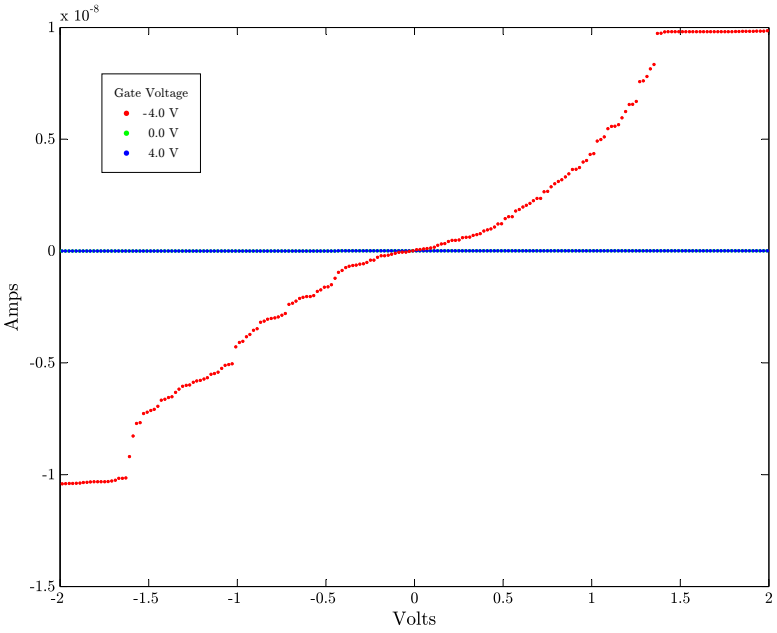

Figure B.24 Device 24.

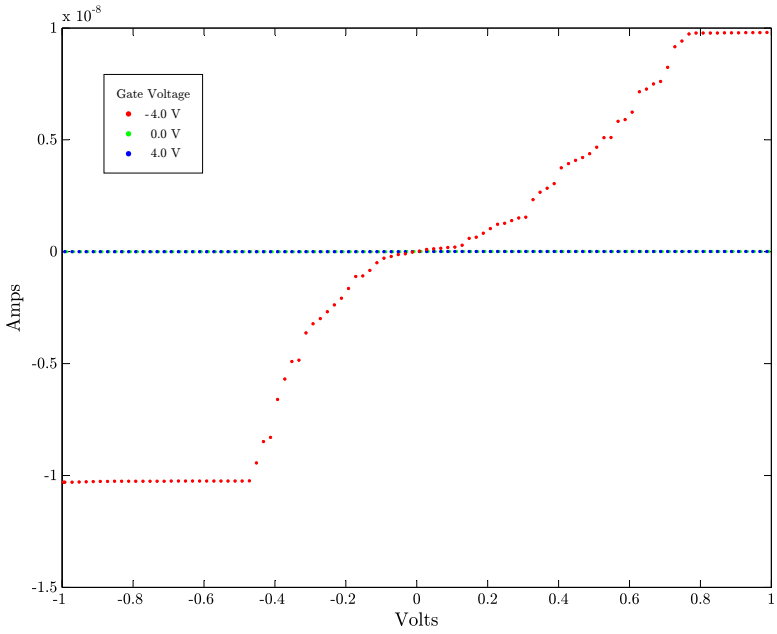

Figure B.25 Device 25.

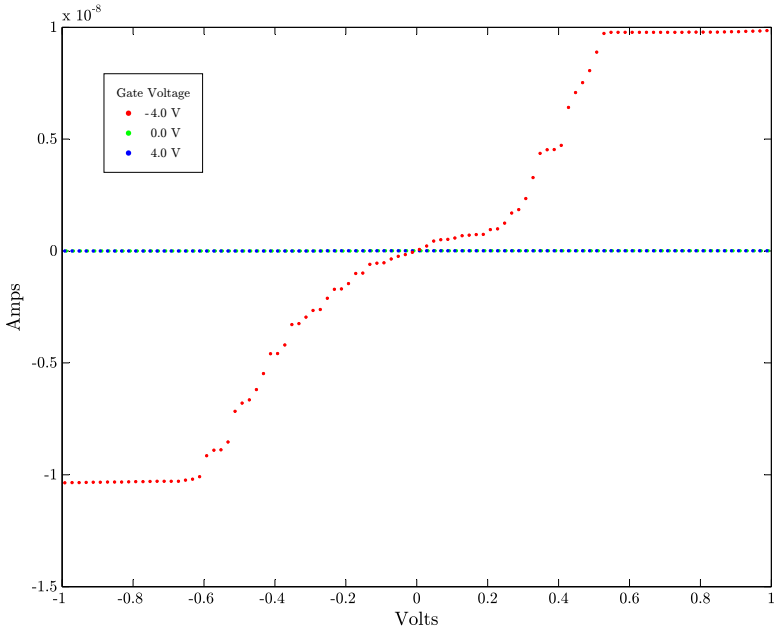

Figure B.26 Device 26.

Appendix C

Gate Voltage Sweep Data

This appendix contains the gate voltage sweep data referred to in this study. The gate voltage was generally varied from -5 V to 5 V with source voltages of ±200-1000 mV. While source voltage sweeps were performed on every device, gate voltage sweeps were only performed on a few.

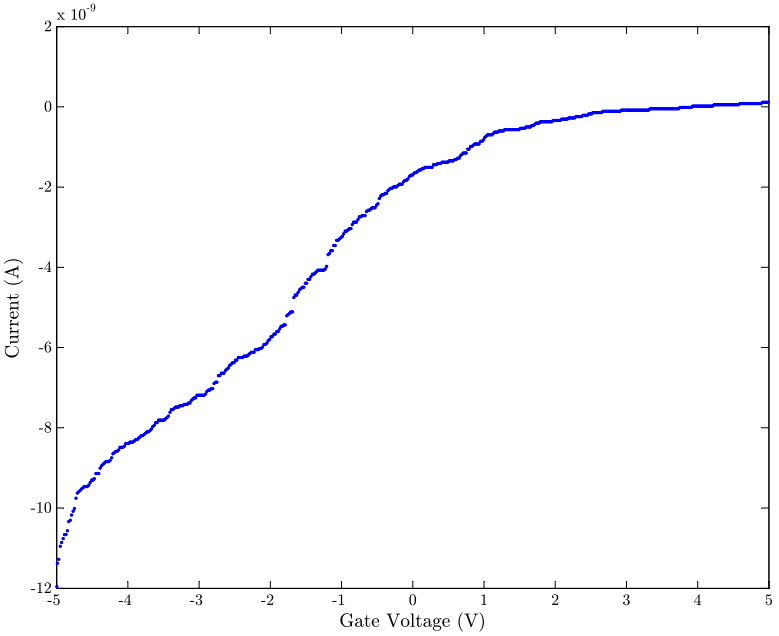

Figure C.1 Device 4 with -1000 mV source-drain voltage.

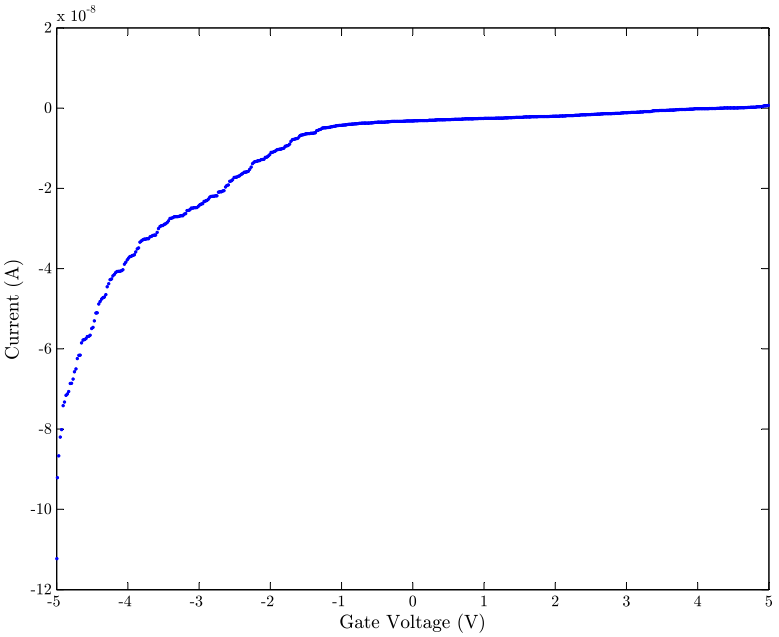

Figure C.2 Device 6 with -1000 mV source-drain voltage.

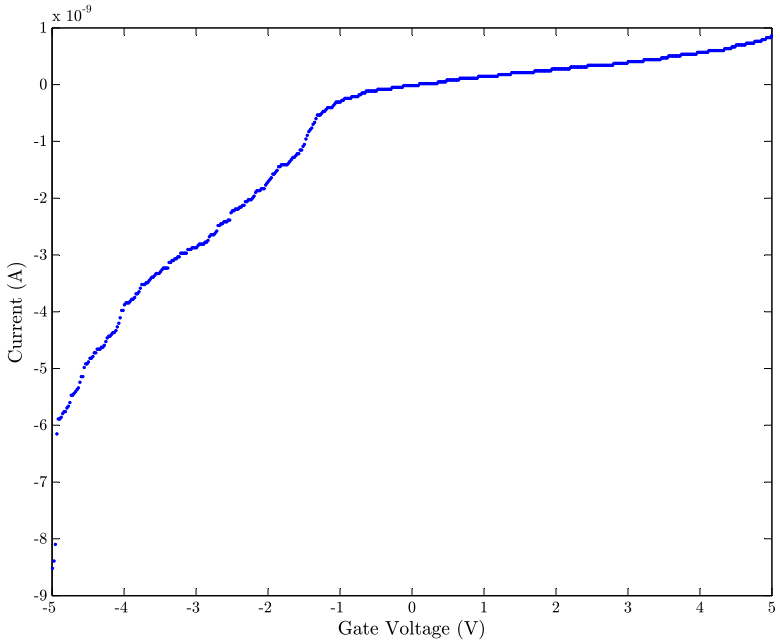

Figure C.3 Device 6 with -800 mV source-drain voltage.

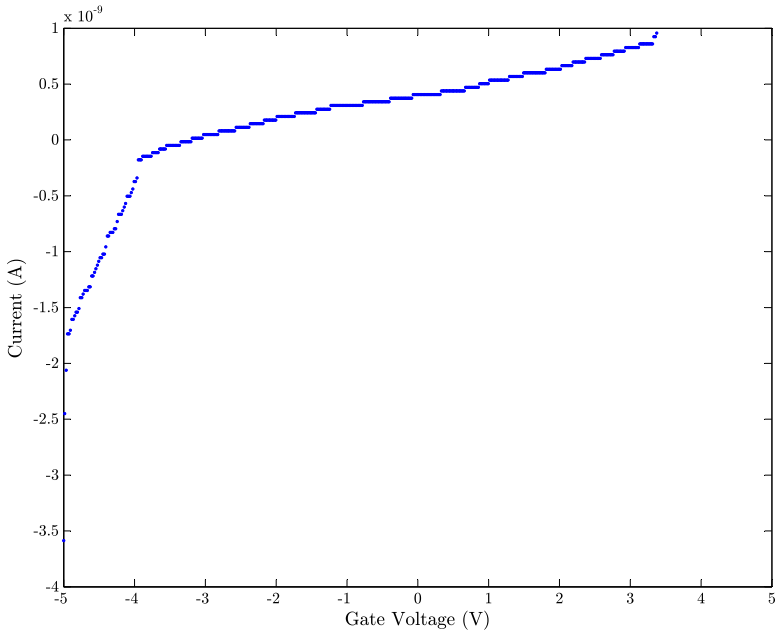

Figure C.4 Device 6 with -600 mV source-drain voltage.

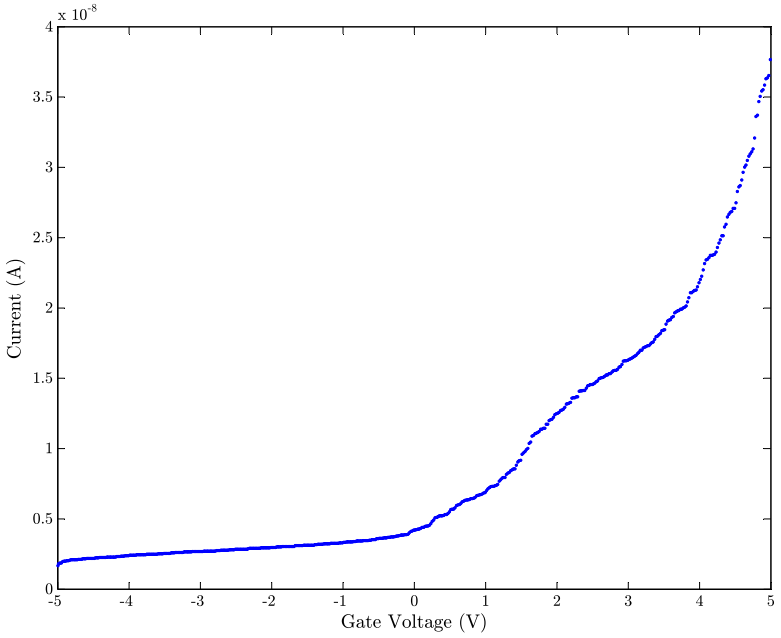

Figure C.5 Device 6 with 200 mV source-drain voltage.

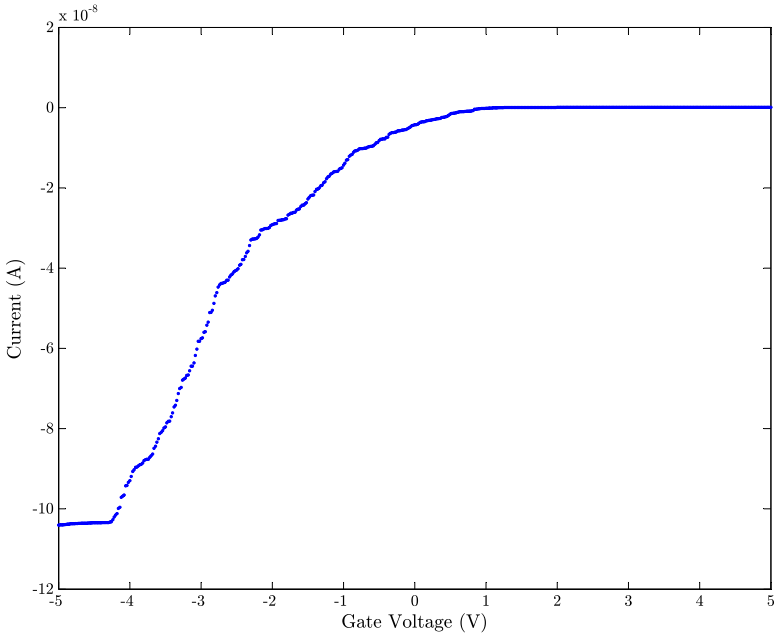

Figure C.6 Device 11 with -1000 mV source-drain voltage.

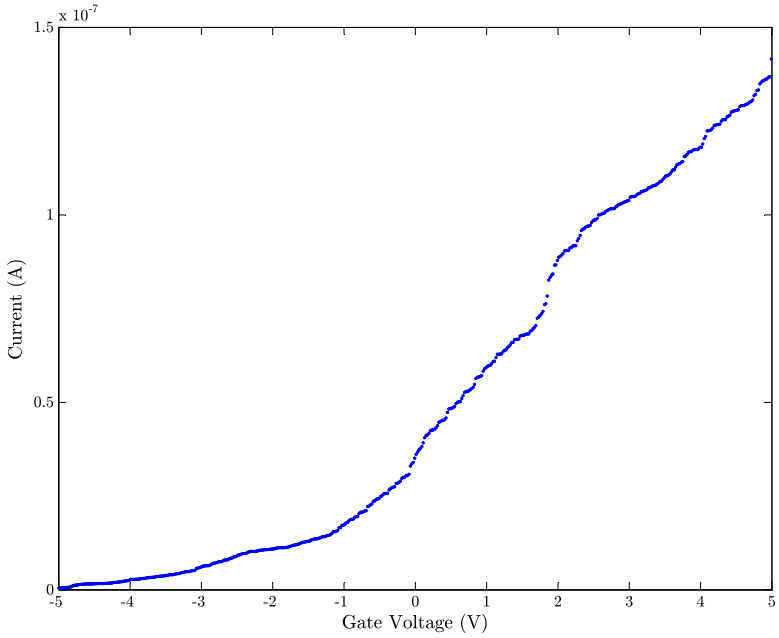

Figure C.7 Device 16 with 500 mV source-drain voltage.

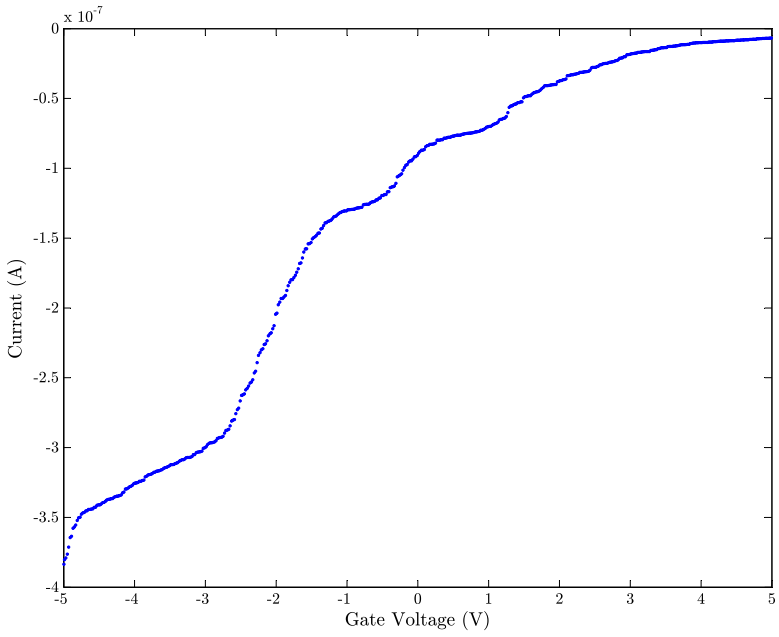

Figure C.8 Device 16 with 600 mV source-drain voltage.

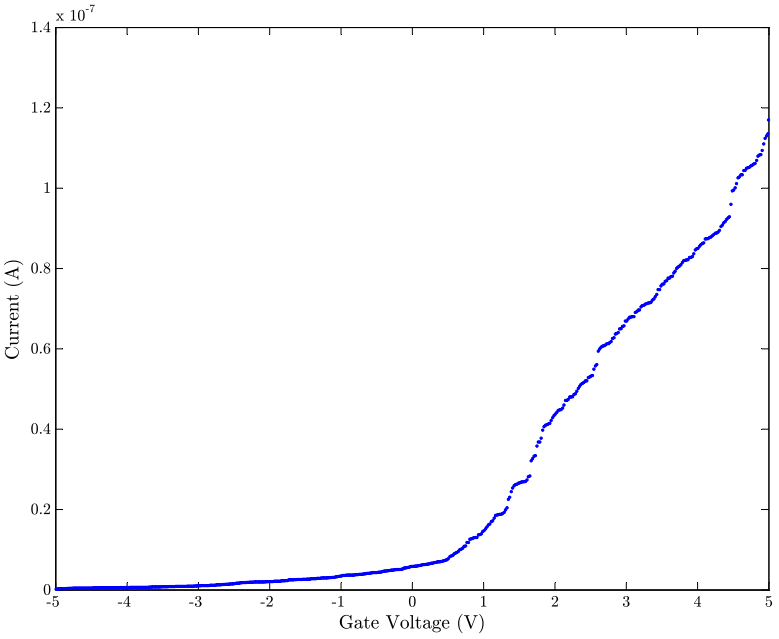

Figure C.9 Device 16 with 1000 mV source-drain voltage.

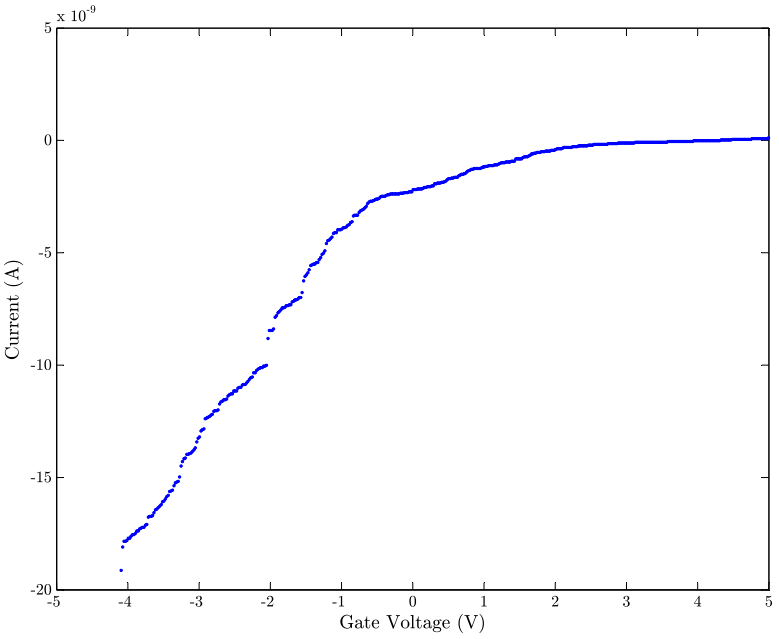

Figure C.10 Device 23 with -1000 mV source-drain voltage.

Appendix D

S.O.P. for Nanotube Purification

This appendix contains a detailed standard operating procedure (S.O.P.) for nanotube purification. It is strongly recommended that those new to centrifugation read the first four chapters of *Biological Centrifugation* by J.M Graham in order to acquire an intuition for the processes described below. In all steps involving ultracentrifugation, tubes must be filled to 80% capacity in order to prevent their collapse during centrifugation.

D.1 Preparation

Each step of the procedure will require one of two solutions. A low density solution is prepared by adding surfactants to water. A high density solution is prepared by adding the same surfactants to a solution of Iodixanol. Each solution is stored at room temperature in tightly sealed glass containers. The quantities outlined below will last for several runs.

Water Solution

1. Fill the container with 100 mL of HPLC grade water.

2. Add 1.6 g (1.6 wt%) sodium cholate hydrate (Sigma-Aldrich C6445).

3. Add 0.4 g (0.4 wt%) sodium dodecyl sulfate (Sigma-Aldrich L6026).

4. Seal the container and agitate until the mixture homogenizes and foaming subsides. This may take several minutes. The resultant solution will be clear.

Iodixanol Solution

1. Fill the container with 100 mL of OptiPrep (Sigma-Aldrich D1556).

2. Add 2.112 g (1.6 wt%) sodium cholate hydrate (Sigma-Aldrich C6445).

3. Add 0.528 g (0.4 wt%) sodium dodecyl sulfate (Sigma-Aldrich L6026).

4. Seal the container and agitate until the mixture homogenizes and foaming subsides. This may take several hours. The resultant solution will have a slightly yellow tint.

D.2 Dispersion

The raw nanotube soot is primarily composed of large nanotube aggregates. Sonication is used to disperse these aggregates into solution. The surfactants will keep the separated nanotubes from recombining.

1. Fill a small glass beaker with 10 mL of water solution.

2. Add 3-5 mg of single-walled carbon nanotube soot (SWeNT SG 76).

3. Suspend the beaker in an ice bath. Be sure to replenish the ice throughout sonication.

4. Insert the horn of the Tekmar Sonic Disrupter (TM 375) about 1/3 of the way into the water solution.

5. Set the sonicator to power 4 with a 30% duty cycle.

6. Sonicate for 2 hours. The solution will begin to darken within the first few minutes and will continue to darken throughout sonication. The resultant solution will be completely black.

D.3 Pelletization

Even after significant sonication, the solution will still contain some nanotube aggregates. The largest of these remaining aggregates are removed using differential centrifugation. The largest nanotube aggregates will form a solid pellet at the bottom of the centrifuge tube, after which the supernatant is easily decanted for further processing.

1. Decant the sonicated solution into 2 small (5 mL, 13 $\times$ 51 mm) Ultra-Clear centrifuge tubes (Beckman Coulter 344057).

2. Transfer liquid between the centrifuge tubes until their difference in weight is less than 0.01 g. This will ensure that the rotor remains balanced during centrifugation.

3. Place the centrifuge tubes into opposing buckets of the SW 55 Ti Rotor (Beckman Coulter 342196). Attach all remaining buckets to ensure proper balance.

4. Set the speed and temperature of the Optima LE-80 K Ultracentrifuge to 41,000 rpm and 22 C.

5. Centrifuge for 30 minutes.

6. Carefully decant the supernatant into a sterile container. Stop decanting before pieces of the pellet are allowed to enter the sterile container. The yield will be about 4.5 mL per centrifuge tube.

D.4 Concentration

During the separation step, it will be important to minimize the distance between the starting point and the isopycnic point of any given nanotube. Thus, the separation step is optimized when the nanotube solution is highly concentrated. Such concentration is achieved using isopycnic centrifugation with a discrete 2-step density gradient. The bottom step acts as a barrier, causing highly concentrated nanotube solution to band at the interface.

1. Fill 2 large (13.2 mL, 14 × 89 mm) Ultra-Clear centrifuge tubes (Beckman Coulter 344059) with 7.5 mL of iodixanol solution.

2. Using a thumb-wheel pipetter, slowly release the nanotube solution on top of the iodixanol layers. To minimize mixing, the centrifuge tube should be angled at 45° with the pipetter held nearly vertical. This allows the liquid to slowly run down the side of the tube before reaching the meniscus. The liquid should be released along the lower inner wall of the centrifuge tube near the meniscus.

3. Transfer nanotube solution between the centrifuge tubes until their difference in weight is less than 0.01 g. This will ensure that the rotor remains balanced during centrifugation.

4. Place the centrifuge tubes into opposing buckets of the SW 41 Ti Rotor (Beckman Coulter 331362). Attach all remaining buckets to ensure proper balance.

5. Set the speed and temperature of the Optima LE-80 K Ultracentrifuge to 41,000 rpm and 4 C. This low temperature is intended to maintain the gradient profile by preventing excessive diffusion.

6. Centrifuge for 15 hours. This will cause the nanotube solution to become concentrated and form a thin black band near the center of the centrifuge tube.

7. Use the BioComp Gradient Station to fractionate the thin black band from each centrifuge tube. The fractionated solution should be stored in a sterile container. Since the tip of the trumpet is not a good indicator of fraction location, it is necessary to mark the desired region on a piece of tape using the cursor. Only then can the tip of the trumpet be used as a guide. The fractionated region should start slightly above the band and end slightly below it. This ensures maximum yield.

D.5 Separation

With the nanotube solution properly homogenized and concentrated, it is ready for separation. This is achieved using isopycnic centrifugation with a continuous 4-step density gradient. The continuous gradient will allow nanotubes of different chiralities to band at their respective isopycnic points.

1. Premix each gradient step in a small glass container according to the specifications below. Aside from the nanotube steps, there will be a total of 4 gradient steps in each centrifuge tube, so 8 separate containers are required. Each step will need to be prepared twice. Be sure to label the containers in order to avoid confusion during the layering process.

    a. Bottom Step

i. 0.553 mL iodixanol solution

ii. 0.447 mL water solution

a. Bottom Middle Step

i. 1.070 mL iodixanol solution

ii. 1.431 mL water solution

a. Top Middle Step

i. 0.440 mL iodixanol solution

ii. 2.060 mL water solution

a. Top Step

i. 0.201 mL iodixanol solution

ii. 3.800 mL water solution

2. Fill 2 large (13.2 mL, 14 × 89 mm) Ultra-Clear centrifuge tubes (Beckman Coulter 344059) with 1 mL of iodixanol solution. This layer acts as a base for the gradient, raising the gradient high enough in the tube so that the fractionator trumpet can reach the important fractions.

3. Using a thumb-wheel pipetter, slowly release each step of the density gradient on top of the previous step. The nanotube solution should be layered between the two middle steps. For each tube, start with the bottom step and end with the top step. To minimize mixing, the centrifuge tube should be angled at 45 with the pipetter held nearly vertical. This allows the liquid to slowly run down the side of the tube before reaching the meniscus. The liquid should be released along the lower inner wall of the centrifuge tube near the meniscus.

4. Tightly seal each centrifuge tube with Parafilm and carefully lay each tube on its side. It is essential that this step be performed with extreme care so as to prevent any mixing.

5. Let the centrifuge tubes sit on their sides for 2 hours. The purpose of this step is to transform the discrete gradient into a continuous gradient by way of diffusion. By laying the tubes on their sides, the surface area between each step is maximized, allowing for a greater amount of diffusion to take place.

6. Carefully raise the centrifuge tubes to a vertical position. It is essential that this step be performed with extreme care so as to prevent any mixing.

7. Place the centrifuge tubes into opposing buckets of the SW 41 Ti Rotor (Beckman Coulter 331362). Attach all remaining buckets to ensure proper balance.

8. Set the speed and temperature of the Optima LE-80 K Ultracentrifuge to 41,000 rpm and 4 C. This low temperature is intended to maintain the gradient profile by preventing excessive diffusion.

9. Centrifuge for 15 hours. This will cause nanotubes of different chiralities to band at their respective isopycnic points. Once the centrifuge comes to a stop, it is essential that the fractionation step be performed immediately, since diffusion will begin as soon as the centrifuge comes to a stop. The centrifuge buckets containing the nanotube solution should be kept in ice while being transported from the centrifuge to the fractionator.

D.6 Fractionation

Each band represents a unique nanotube species. A fractionator is used to extract fractions of these bands while minimizing mixing between them. For detailed instruc-

tions on operating the fractionator, refer to the BioComp manual.

1. Remove one of the centrifuge tubes from its bucket.

2. Attach a ruled sticker along the length of the tube with zero at the top of the tube.

3. Using the ruled sticker, determine the zone of interest and attach thin strips of brightly colored tape at the beginning and end of the zone of interest.

4. Insert the centrifuge tube into the holder of the BioComp Gradient Station. Be sure that the brightly colored markers are visible through the viewing window. Since the holder uses only friction to hold the centrifuge tube in place, it is sometimes necessary to add a band of porous tape around the top of the tube, providing more grip for the holder.

5. Set the BioComp Gradient Station to automatically fractionate in increments of 0.5 mm.

6. Since the tip of the trumpet is not a good indicator of fraction location, it is necessary to mark the desired region on a piece of tape using the cursor. Only then can the tip of the trumpet be used as a guide.

7. Begin the automated fractionation. The fractions will consist primarily of foam since the fractionator aerates the surfactant-rich solution. Thus, the centrifuge tubes in this step should be large enough to accommodate large amounts of foam (approximately 15 mL). The centrifuge tubes should also be of standard size so that they fit in a conventional low-speed tabletop centrifuge.

8. Use a low-speed tabletop centrifuge to condense the foam of each fraction into liquid. This step prevents nanotube solution from drying up on the sides of the

centrifuge tube.

9. When fractionation is complete, dilute each fraction with 5.0 mL of water solution. Using the surfactant-rich water solution will prevent aggregates from forming in the solution.

10. The fractions are now ready for use. It is wise to gently sonicate each fraction in a bath sonicator prior to optical analysis or electrical measurement, as this will minimize the number of aggregates in the solution.